Deep–Sea Research II 189-190 (2021) 104952

Contents lists available at ScienceDirect

Deep-Sea Research Part II

journal homepage: www.elsevier.com/locate/dsr2

Spatial and temporal variability of dissolved aluminum and manganese in surface waters of the northern Gulf of Alaska

Anna Kandel *, Ana Aguilar-Islas

College of Fisheries and Ocean Sciences, University of Alaska Fairbanks, AK, USA

ARTICLE INFO

Keywords:
Trace elements
Northern Gulf of Alaska
Dissolved manganese
Dissolved aluminum
Subpolar
River plume
Chemistry
Profiles
Elements (chemical)

ABSTRACT

The Northern Gulf of Alaska (NGA) shelf is a productive high-latitude environment where nutrient dynamics are greatly impacted by the seasonal variability in freshwater input. Iron is a key nutrient on the NGA shelf that directly modulates primary production, and freshwater is a major input of iron to the NGA shelf. However, variability in the input of dissolved iron from freshwater sources is obscured by high biological uptake and by the concentration of organic ligands, which bind iron and help maintain it in solution. Riverine inputs of other lithogenic elements such as aluminum and manganese are expected to behave quasi-conservatively on the NGA shelf and could help provide insight into the variability of iron input in this region.

Here we present the seasonal (spring, summer, and fall) distribution of dissolved aluminum (dAl) and manganese (dMn) observed during 2018 and 2019 in the NGA region. Data were obtained during the NGA Long Term Ecological Research (LTER) site cruises and include several surface transects from Kayak Island to Kodiak Island, vertical profiles at several locations sparsely distributed throughout the shelf, and surface information from a Copper River plume study. We find that seasonal patterns in the surface concentrations of dMn and dAl mirrored annual glacial melt cycles, with the lowest values observed in spring and higher values in summer and fall. Sharp cross-shelf gradients were observed for both metals particularly in summer and fall. Surface concentrations decreased (by 1–2 orders of magnitude) away from the outflow of the Copper River, the major point source of freshwater within the NGA LTER site. Extremely high concentrations in the Copper River plume ($\leq$1395 nM dAl, $\leq$128 nM dMn) and strong correlations with salinity ($p = 7.9E\text{-}14$ for dAl, 1.4E-14 for dMn) highlight the quasi-conservative nature of these metals within the plume. Enhanced dAl and dMn concentrations within nepheloid layers in subsurface waters indicate regions where a sedimentary source of iron could also be important. Residence times for dAl and dMn in surface waters over the NGA shelf were estimated to be 31 days (dAl) and 42 days (dMn) on average based on summer and fall data from both years.

1. Introduction

The Northern Gulf of Alaska (NGA) shelf is a productive high-latitude ecosystem characterized by intense environmental variability including a complex bathymetric setting, high seasonality in freshwater input due to snow and glacier melt (Royer 1981), and an irregular cross-shelf water mass distribution set by changing local wind patterns (Royer 1975) and the presence/absence mesoscale eddies (Ladd et al., 2007). This environmental setting leads to variable macro- and micronutrient fields that contribute to a spatial and temporal patchwork in primary production (Strom et al., 2006), which is further modulated by strongly variable light conditions (Strom et al., 2010).

Insight into the variable freshwater input of trace elements into a coastal system can be gained from the surface distributions of dissolved aluminum (dAl) and manganese (dMn) in plume waters, given freshwater is a dominant source for these lithogenic elements (e.g., Hydes 1979; Orians and Bruland 1986). Further insight into removal (e.g., scavenging) and other inputs (e.g., photoreduction) within surface shelf waters can be inferred from deviations from conservative mixing with respect to salinity, although calculated riverine endmembers can vary depending on season (Guieu and Martin 2002), tidal amplitude (Aguilar-Islas and Bruland 2006), and setting. For example, seasonal differences in averaged riverine endmember dAl and dMn values reported for the Danube River (Guieu and Martin 2002) ranged from ~210 to 540 nM for dAl and ~25–55 nM for dMn. Tidal amplitude has been shown to contribute to the variability in riverine endmembers for dMn in the

* Corresponding author.
E-mail address: arykandel@gmail.com (A. Kandel).

https://doi.org/10.1016/j.dsr2.2021.104952
Received 17 February 2021; Received in revised form 28 June 2021; Accepted 21 July 2021
Available online 27 July 2021

Columbia River (~550 nM during spring tide conditions compared to ~110 nM during neap tides) (Aguilar-Islas and Bruland 2006). Finally, ranges of dAl calculated for the riverine endmembers can vary by several orders of magnitude for glacially-fed rivers, such as the Copper and Alsek (>1700 nM) (Brown et al., 2010), compared to temperate rivers like the Yangtze and Columbia Rivers (~85 nM and 220 nM, respectively) (Ren et al., 2006; Brown et al., 2009).

In the NGA, seasonal variability in riverine endmember concentration along with seasonality in freshwater input (Royer 1981) is expected to lead to the lowest trace metal concentrations in winter/spring when glacial melt is minimal, and to a more discernible seasonal pattern in surface trace metal distribution in regions impacted by large freshwater point sources such as the Copper River. Besides freshwater influences, tidal mixing over shallow banks and storms can break surface stratification and alter surface trace metal concentrations by entraining subsurface waters with different dissolved metal signatures. Additionally, upwelling/downwelling conditions have been shown to influence trace metal concentrations in buoyant plumes (e.g., Aguilar-Islas and Bruland 2006; McAlister and Orians 2012).

One of the goals of the NGA LTER site is to investigate how intense environmental variability can lead to ecosystem resilience. The wide ranges of dAl (Brown et al., 2010) and dFe (Lippiatt et al., 2010; Aguilar-Islas et al., 2016) values previously observed in the NGA are likely modulated by, and contribute to, the environmental variability. Here we investigate the seasonal distribution of dAl and dMn throughout the NGA study region to gain insight into the various processes influencing the input of trace metals into the Gulf of Alaska and provide information about the seasonality of this input, as variability in surface trace metal values has the potential to moderate primary production in the NGA shelf (Strom et al., 2006; Aguilar-Islas et al., 2016).

1.1. Physical setting

The Gulf of Alaska (GOA) is surrounded by the Alaskan coastline to the north, east, and west, while to the south it borders the high-nutrient, low-chlorophyll (HNLC) waters of the subarctic North Pacific. The NGA as defined by our study area within the Gulf consists of three transects that start along the coast between the Copper River delta (145 °W) to the eastern edge of Kodiak Island (152 °W) and extend offshore into the slope, as well as stations within Prince William Sound. Major circulation in the GOA is driven by the Alaska Gyre in the ocean basin and the Alaska Coastal Current (ACC) over the shelf (Fig. 1). Gyre circulation in the GOA includes the Alaska Current, which moves northward following the contour of the continental shelf break and turns southwest at the northernmost extent of the Gulf, becoming the Alaskan Stream (Royer and Emery 1987; Lagerloef 1995). On the inner portion of the continental shelf, the ACC is separate from gyre circulation and is driven by wind and freshwater input, with speeds up to 175 cm/s (Schumacher et al., 1989; Weingartner et al., 2005). It flows westward along the southern coast of the Kenai Peninsula, likely splitting around Kodiak Island.

The pressure system over the NGA shelf is dominated by the Aleutian Low for most of the year, leading to strong downwelling from fall-spring. In summer the Aleutian Low may be displaced by the North Pacific High leading to a relaxation of the downwelling winds and thus weak upwelling (Royer 1975). The NGA also experiences intense seasonal variability in freshwater input, mainly due to the melt cycles of glaciers which encompass an area of >72,000 km^2 in the GOA watershed (Beamer et al., 2016) as well as seasonal changes in precipitation (Hill et al., 2015). Glacial melt peaks in early autumn as a direct result of higher temperatures in the warm season, which is often defined as the period from May–October or June–November, and during which runoff has been shown to double compared to the rest of the year (Royer 1981).

2. Materials and methods

2.1. Sample collection

Seawater samples were collected during 6 cruises (spring, summer, and fall) in 2018 and 2019. Cruise dates and vessels are shown in Table 1. Cruises sampled established NGA LTER stations along the historic Seward Line (GAK), the Middleton Island Line (MID), and the Kodiak Line (KOD), as well as stations throughout Prince William Sound (PWS). Additional transects were sampled during the summer 2019 cruise to study the Copper River plume (7/3/19–7/8/19). Surface sampling (~1 m) was conducted with a towed surface pump "Fe fish" system modified from that described in Aguilar-Islas and Bruland (2006). The modified system is comprised of an air-actuated PTFE diaphragm pump (Wilden) and PFA Teflon™-lined tubing attached to a bathythermograph. In rough conditions a secondary 20 kg PVC torpedo was added to keep the Fe fish below the surface and prevent

Table 1
Cruise vessels, dates, and IDs for all 2018 and 2019 NGA LTER cruises.

Season	Vessel	Dates	Cruise ID
Spring 2018	R/V Sikuliaq	4/18–5/5	SKQ201810S
Summer 2018	M/V Wolstad	7/3–7/18	WOL201807
Fall 2018	M/V Tiglax	9/11–9/25	TGX201809
Spring 2019	M/V Tiglax	4/26–5/9	TGX201904
Summer 2019	R/V Sikuliaq	6/27–7/17	SKQ201915S
Fall 2019	M/V Tiglax	9/11–9/25	TGX201909

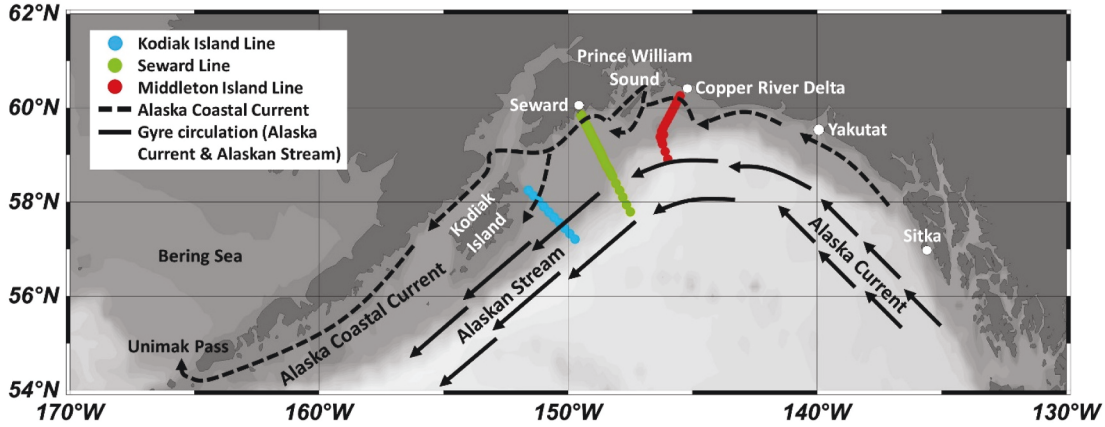

Fig. 1. Major circulation in the GOA with bathymetry contours at 100 m, 250 m, 500 m, 1000 m, and 5000 m. The Kodiak, Seward, and Middleton Lines sampled in this study are also shown.

"porpoising" while towing. The Fe fish was deployed from the starboard side of the vessels and towed at speeds of 6–10 knots depending on conditions, allowing for clean underway surface water sampling. On all cruises except TGX201904 (spring 2019), underway salinity data were acquired via a YSI Sonde positioned in the clean lab space inside a plastic cylinder from the overflow of the Fe fish system.

Surface samples taken for dissolved aluminum and manganese analysis were filtered in-line through a 0.2 μm filter cartridge (Supor Acropak 200, Pall Corporation) and collected in acid-cleaned, 100 mL, low density polyethylene (LDPE) bottles (Bel-Art). New filter cartridges were initially rinsed in-line with at least 5 L seawater prior to use, and then with 0.5 L seawater before taking each sample. When possible, a single filter cartridge was used per sampling line by storing cartridges emptied of seawater in a plastic bag and refrigerating overnight.

Depth profiles could not be obtained from cruises on M/V Tiglax and M/V Wolstad due to lack of required deployment equipment on those vessels. Therefore, vertical profiles were obtained only from cruises SKQ201810S (spring 2018) and SKQ201915S (summer 2019) using a trace metal clean 12-bottle rosette (TMCTD) as described in Rember et al. (2016). The rosette is a powder-coated aluminum frame fitted with a Sea-Bird Electronics 19plus profiler for conductivity, temperature, and depth (CTD) measurements, a Wet Labs EcoView fluorometer, a Wet Labs C-star transmissometer, and a Sea-Bird Electronics auto fire module (AFM) to close bottles at pre-programmed depths. The bottles are Teflon™-coated 5 L Niskin-X bottles (General Oceanics and OceanTest Equipment) with Teflon™-coated external springs. They were washed prior to the cruises with dilute trace metal grade hydrochloric acid (TMG HCl) and ultrapure Milli-Q (MQ) water and stored with MQ water for 1 month, and then stored emptied until used. An AmSteel™ line and a trace metal-clean block were used during deployment to prevent contamination. Following recovery, the bottles were transferred to a plastic enclosure with positive pressure, seawater was filtered through 0.4 μm polycarbonate filters (Nuclepore) mounted on Teflon filter holders (Savillex), and samples were collected in acid-cleaned 125 mL high-density polyethylene (HDPE) bottles. To increase filtering speed the Niskin bottles were pressurized with ultrapure nitrogen gas (5 psi) (the tank was kept outside the plastic enclosure). Aluminum bar clamps were used to hold the Niskin bottles closed while the gas was on, and the metal bars were covered with electrical tape to prevent contamination.

2.2. Sample processing

Seawater samples were stored at room temperature and acidified with Optima grade concentrated HCl (2 mL HCl/L) to ~pH 1.7 upon return to the laboratory. Due to wide ranges of dAl and dMn values, samples with high concentrations (operationally defined here as >70 nM Al, >20 nM Mn) were diluted prior to analysis, while samples with concentrations below those thresholds were concentrated onto a column as detailed below.

Samples with high concentrations of dAl and dMn were diluted into 15 mL Teflon™ tubes using 0.13 mL sample, 3.77 mL 2% Optima-grade nitric acid (HNO_3), and 0.1 mL indium (In) spike (40 ppb in 2% Optima-grade HNO_3). Combined aluminum and manganese standards were made in 2% Optima-grade HNO_3 with concentrations of 0, 5, 10, 20, and 40 nM Al and 0, 1, 3, 5, and 10 nM Mn. To ensure matrix matching between standards and samples, solutions containing 0.13 mL low-aluminum seawater (<5 nM), 3.77 mL standard, and 0.1 mL In spike were prepared immediately prior to analysis.

Samples with low concentrations of dAl and dMn (operationally defined here as <70 nM Al, <20 nM Mn) were preconcentrated in an offline, flow-through system consisting of two 6-port, 2-position valves (VICI) and a 12-position actuator valve (VICI) that functioned as an autosampler (Fig. 2). A column packed with NOBIAS Chelate-PA1 resin was used to concentrate trace elements and remove major salts and ammonium acetate was used to modify sample pH prior to column loading. Samples were eluted with 10% optima-grade HNO_3, and Milli-Q water (MQ) was used as the column conditioner. Eluted solutions were collected into 8 mL acid clean LDPE bottles. The ammonium acetate solution was prepared with a 10:7:33 ratio of optima-grade ammonium hydroxide, glacial acetic acid, and MQ to achieve pH 5.5–6 in the sample-buffer mixture, previously determined to be ideal for retention of both Al and Mn (Minami et al., 2015). Ratios between the sizes of pump tubing (and thus flow rates) are comparable to those used in Brown and Bruland (2008) except for the eluent tubing, for which a larger size was used.

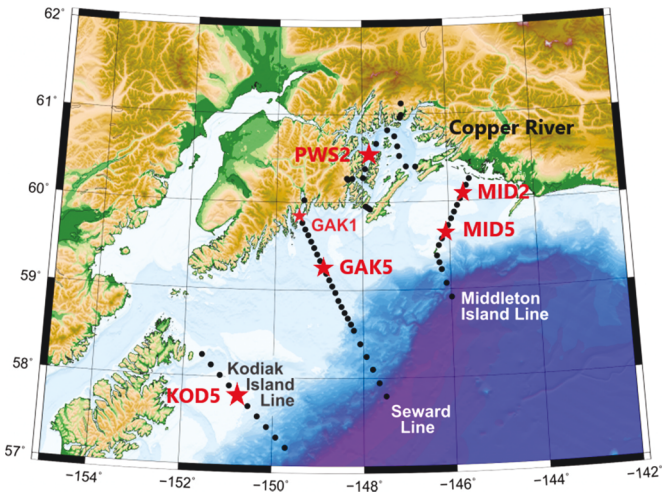

Fig. 2. Map of sampling sites in the Northern Gulf of Alaska showing the KOD, GAK, and MID Lines as well as sites within Prince William Sound. Red stars indicate stations with vertical profiles of dAl and dMn. LTER cruises took place during spring, summer, and fall in 2018 and 2019, sampling every line on every cruise (weather permitting).

Combined dAl and dMn standards were prepared in a 50/50 (by weight) solution of MQ and filtered low-aluminum seawater (<5 nM dAl) collected from offshore in the NGA during the summer 2019 cruise and acidified with optima grade HCl (2 mL HCl/L). Aluminum standard concentrations were 0, 1, 5, 10, 15, 25, 40, 55, 70, and 80 nM, and Mn standard concentrations were 0, 0.1, 0.5, 1, 3, 5, 9, 12, 15, and 20 nM. Pump tubing (Fisher Scientific; ALPKEM) was replaced after four days of use, or approximately every 120 samples. Up to 10 days prior to use new tubing was filled with 10% trace metal grade (TMG) HCl (Fisher Scientific) which was changed every couple days to ensure thorough cleaning.

The manifold setup was based on that used in Brown and Bruland (2008), with two 6-port, 2-position valves, and our setup also included a third 12-position valve that was used as an autosampler. All valves were controlled using VICI VCom software. The system was cleaned immediately prior to use with 0.1% optima grade HCl. A blank equivalent to the 0 nM std was used to check the pH of the sample-buffer mixture at the beginning of each day. If the pH was too low, additional optima grade NH_4OH was added to the ammonium acetate solution. To condition the column with seawater the blank was then loaded and eluted for 2 min each, and this cycle was run 5 times. The preconcentration program started with a 15 s rinse of the tubing and column, followed by a sample loading time of 7.25 min, a second 15 s rinse, and an elution/collection time of 1.25 min.

A set of 5 standards was chosen for each day based on expected dAl and dMn values of the samples, estimated either by using the dilution method first or by comparison to geographically and temporally nearby samples that had already been quantified. Standards were collected in duplicate before samples were run. Standards were run in decreasing order from highest concentration to lowest because we found additional salts on the column further cleaned it, and this facilitated accurate quantification of the lowest standard. Carryover was not an issue, as the

column eluted completely during the elution time. Every twelfth sample was run in duplicate, and all other samples were run only once.

2.3. Analysis

Analyses were performed at the University of Alaska Fairbanks by inductively coupled plasma mass spectrometry (ICP-MS) using an Element 2 (Thermo-Finnigan) run at medium resolution. Table 2 shows figures of merit. The dilution method blanks consisted of 3.9 mL 2% HNO_3 and 0.1 mL In spike (n 10), and the preconcentration method blanks were MQ water acidified in the same manner as the seawater samples (2 mL HCl/L) and run through the offline preconcentration system (n 7). The blank values were subtracted from samples. The limit of detection (LOD) for the various methods was determined from the standard deviation of the blanks (3), and the precision of each method was determined from the median of the relative standard deviation (%) of the various replicate samples run during the analysis.

To assess the accuracy of methods, certified reference materials CASS-6 (n 3) and NASS-7 (n 3) were analyzed. Only dMn values could be compared to certified values provided in Yang et al., 2018 (Table 3) as dissolved Al values are not published for these materials. Based on the expected dMn concentrations CASS-6 was processed using the dilution method and NASS-7 was processed using the preconcentration method. The obtained dMn values (reported as mean 1 standard deviation) were within the certified ranges.

2.4. Residence time calculations

Residence times for dAl and dMn in surface waters relative to the input from the Copper River were estimated for the shelf area in the vicinity of the Copper River outflow for individual seasons with sufficient surface dissolved metal data. (Table 4). Freshwater input was estimated using USGS Copper River discharge data, averaging the daily discharge means from the 3 days immediately before and during our occupation. Linear relationships between dAl or dMn and salinity (Fig. 16) were used to extrapolate to the zero-salinity endmembers for each season (Brown et al., 2010). Shelf dimensions of 50 km length and 100 km width were chosen to encapsulate the shelf area between Hinchinbrook and Kayak Islands, as well as a mixed layer depth of 10 m. To calculate dAl and dMn reservoirs the geometric means of surface water values between MID1-MID6, and values over the shelf from the plume study were used.

3. Results

3.1. Kodiak Island line (KOD)

Surface temperatures on the KOD Line exhibited an increasing cross-shelf gradient during all occupations of the line (Fig. S1a). Weather prevented sampling past KOD7 (57.55 °N) during fall 2019, and during summer 2019 trace metal sampling along this line was not completed due to time constraints. As expected, the lowest temperatures were sampled during spring, and at this time of year cross-shelf gradients were diminished. On average, warmer waters were sampled across the line during all seasons in 2019 (spring ~1.2 C; summer ~ 2.4 C; fall ~0.1 C) relative to 2018.

Surface salinity values were relatively elevated and showed little cross-shelf variability during spring, while cross-shelf salinity gradients were most pronounced during fall (Fig. S1b). Summer salinity values (~31.7 32.6) were more similar to those observed in spring (~32.2 32.6) than those in fall (~30.2 31.4). This suggests that diversion of ACC waters to the offshore side of Kodiak Island may be more common during fall than summer. This is unlike the Seward and MID Lines (Sections 3.2 and 3.3), which exhibited the low-salinity ACC signature year-round.

Patterns in dAl and dMn distributions along the KOD Line were broadly similar, exhibiting clearer cross-shelf gradients in fall than in summer or spring. The highest dAl values on the KOD Line (as high as 48.2 nM) were observed during fall 2018 at inshore stations, with values generally decreasing offshore (Fig. 3). Fall 2019 dAl values also tended to decrease from inshore to offshore, but values were lower (maximum 28.3 nM) although salinity ranges were similar during both years. The lack of distinct cross-shelf patterns during summer and spring transects is consistent with the narrower range in salinity from KOD1 to KOD10 (57.2 °N) during those seasons. In spring 2019, dAl values were higher in the mid and outer shelf compared to the inner shelf and margin waters. The lowest dAl values were observed over the shelf during summer 2019, and over the shelf dMn was also lowest during summer 2019 and highest in fall 2018. Offshore of KOD6, the temporal variabilities in dAl and dMn were minimal. Along the KOD Line dMn concentrations ranged from 0.9 nM offshore to a maximum of 14.4 nM inshore (fall 2018) (Fig. 3), while the range for dAl was broader, from values below our detection limit during summer 2019 to 48.2 nM (inshore fall 2018).

Some degree of conservative mixing between fresher inshore water and saline waters was observed for dAl and dMn along the KOD Line (Fig. 4). The slope of the mixing line in fall 2018 was roughly twice as steep as that of fall 2019 for both metals. During summer and spring when freshwater influence was diminished along this line, the linear relationship between metal concentrations and salinity decreased. Other inputs and losses likely exerted a greater influence on the distribution of dAl and dMn during these seasons. Four linear regression lines in Fig. 4a and b are not statistically significant (0.05): dAl vs. salinity summer 2018, and summer and fall 2019, and dMn vs. salinity summer 2019.

3.2. Seward Line (GAK)

Similar to the KOD Line, surface temperatures along the Seward Line showed clear differences between spring (cooler) and summer/fall. Water temperatures during spring and summer 2019 were higher on average than the same seasons in 2018 by 0.43 C and 3.76 C

Table 2
MQ blank values, system LODs, precision (mean RSD), and median RSD for both methods of sample processing. System LOD values are based on blanks and method precision are based on the median of the RSD for samples that were run in duplicate.

	Dilution method		Preconcentration method	
	Al	Mn	Al	Mn
Blanks (nM)	30.5 12.5	0.65 0.11	10.7 2.6	0.97 0.05
System LOD (nM) (3)	37.6	0.33	7.8	0.15
Method PrecisionRSD	13.5%	10.0%	23.8%	4.3%

Table 3
Dissolved Mn values obtained for CASS-6 and NASS-7 reference materials compared to the certified values (Yang et al., 2018).

	CASS-6	NASS-7
Method	Dilution	Preconcentration
dMn Average (nM)	38.21 0.55	13.90 0.63
Accepted Range (nM)	39.68 2.18	13.47 1.09

Table 4
Residence times for dAl and dMn in surface waters over the shelf in the Northern Gulf of Alaska from ~144.4 °W to ~146.4 °W.

	dAl	dMn
Summer 2018	~14 days	~23 days
Summer 2019	~5 days	~10 days
Fall 2018	~75 days	~88 days
Fall 2019	~30 days	~46 days
Overall avg.	31 days	42 days

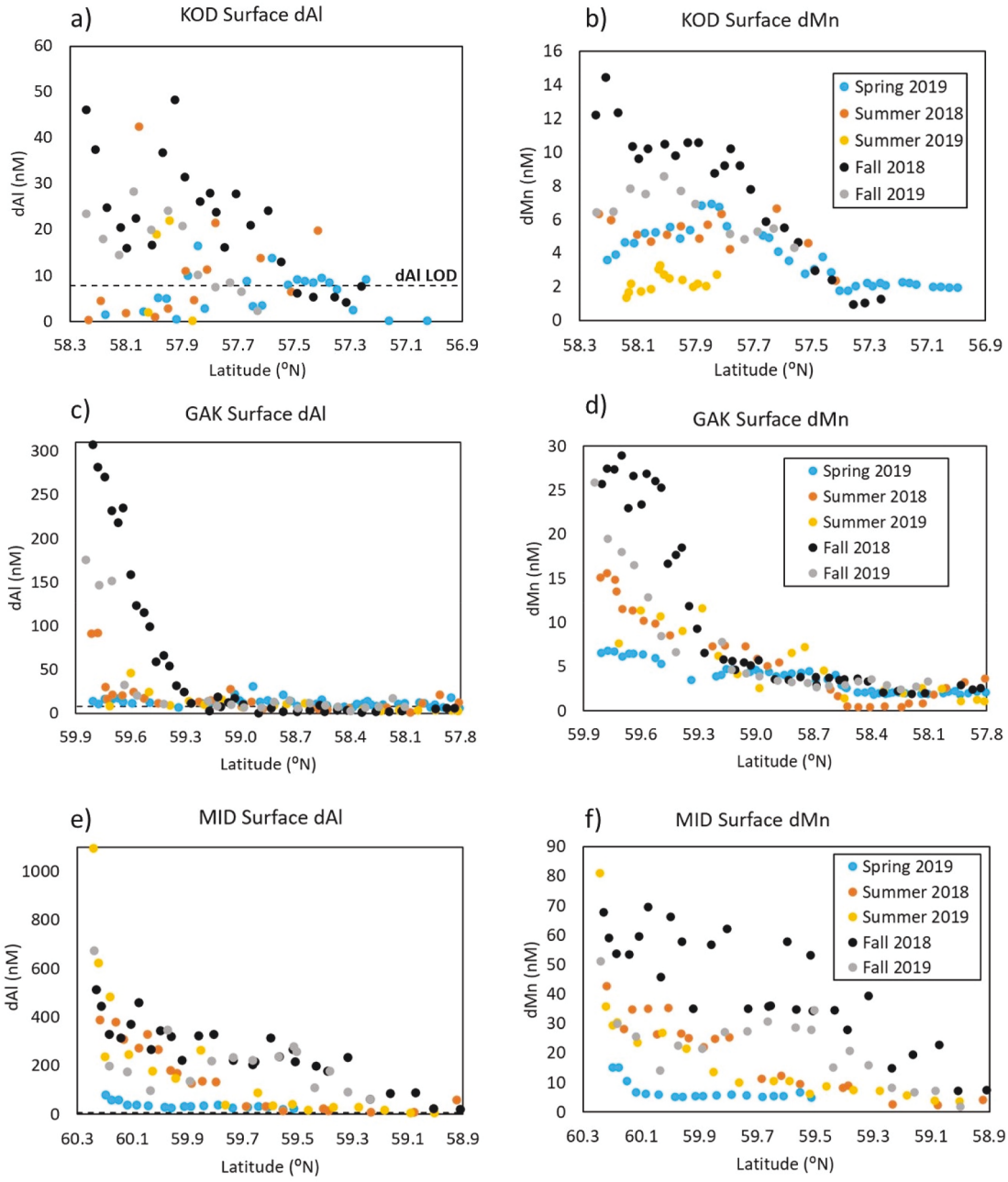

Fig. 3. Dissolved Al and Mn along the KOD Line (a, b, respectively), the Seward Line (c, d, respectively) and the MID Line (e, f, respectively) for all 2018 and 2019 cruises except for spring 2018. All data are shown, and the lines in (a), (c), and (e) at 7.8 nM dAl show the limit of detection (LOD) for dAl. All dMn points were above the LOD. Note that y-axis scales vary.

respectively (Fig. S2a). Fall 2018, however, exhibited warmer surface water than fall 2019, likely as a result of enhanced mixing by storms that impacted the region during our 2019 field campaign. Inshore/offshore temperature differences were less pronounced along the Seward Line compared to the KOD Line.

Cross-shelf gradients in surface salinity were especially pronounced in summer and fall (Fig. S2b). During spring, salinity ranged from about 31.2 to 32.6, and by summer salinity at GAK1 had decreased to the high 20s and then by fall further into the mid and low 20s. The rapid decrease of surface salinity at inshore stations during summer and fall delineates the region that freshwater tends to be constrained to by coastal circulation (the ACC). Interannual salinity differences were more pronounced from GAK1 to GAK4, with fall 2018 being fresher than fall 2019 along these shelf stations. The greater surface salinity in fall 2019 over the shelf supports the notion of enhanced mixing by the storms that coincided with our cruise.

Strong cross-shelf gradients in dAl were apparent along the Seward Line (Fig. 3). The strongest gradient was observed during fall 2018 with the highest value (307.1 nM) furthest inshore followed by a decrease to about 10.8 nM around 59.25 °N. Further south along the line relatively similar concentrations were observed, and concentrations within the same range (≤10 nM) were observed offshore during all seasons. Lower dAl concentrations in fall 2019 compared to the previous year likely resulted from the enhanced storm mixing over the shelf.

Cross-shelf gradients and seasonal variability within the inshore stations were also observed for dMn (Fig. 3). The lowest concentrations were observed in summer 2018 between 58.1 °N and 58.6 °N, while the highest concentrations were observed inshore during fall 2018. During

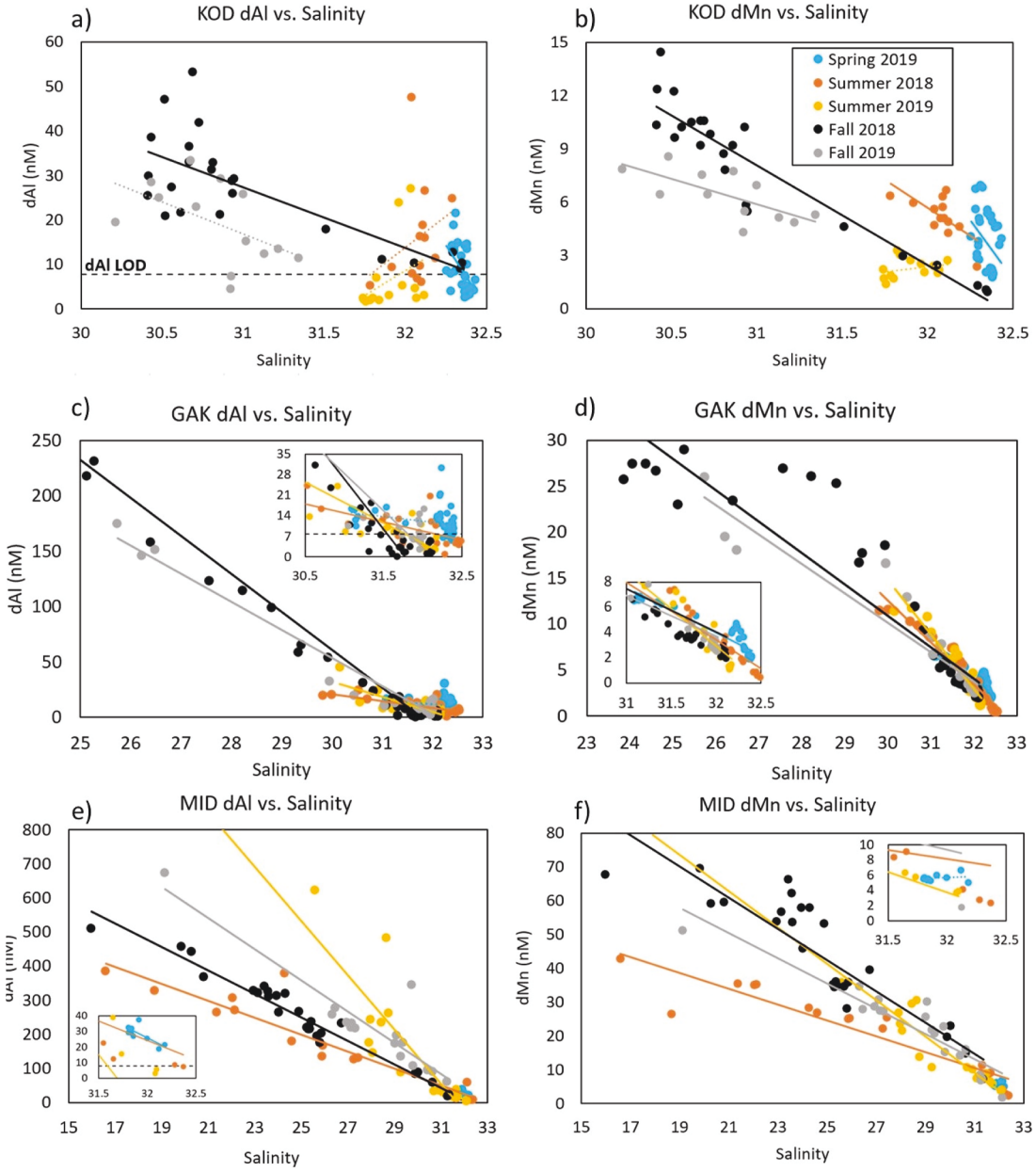

Fig. 4. Dissolved Al and dMn as a function of salinity along the KOD Line (a, b, respectively), the Seward Line (c, d, respectively), and the MID Line (e, f, respectively) on all 2018 and 2019 cruises except for spring 2019. Inserts in (b), (c), and (e) highlight spring 2019 samples with low dAl and dMn. All data are shown, and lines in (a) and the inserts in (c) and (e) at 7.8 nM dAl show the LOD. All dMn data are above the LOD. Solid trendlines indicate relationships that are statistically significant ($\alpha = 0.05$) and dotted trendlines indicate those that are not. The legend in (b) applies to all graphs in this figure.

all seasons dMn fell below 5 nM south of 58.5 ºN. The ACC, mid to outer shelf waters, and margin waters are well delineated by the distribution of dMn along the Seward Line (Fig. 3d). In general dAl concentrations along the Seward Line were an order of magnitude higher than dMn.

Linearity in the relationship between dAl and salinity increased from spring to fall along the Seward Line (Fig. 4). In contrast dMn concentrations exhibited a high degree of linearity with salinity during all seasons, with the most clearly defined conservative mixing line between fresh and saline waters observed in summer (Fig. 4). Differences between the KOD and Seward Lines in these plots illustrate the decreasing influence of freshwater along the ACC, and its influence on surface dAl and dMn. The relationships of dMn and dAl vs. salinity on the Seward Line were statistically significant ($\alpha = 0.05$) during all seasons, except for dAl vs. salinity in spring 2019 (Fig. 4).

3.3. *Middleton Island Line (MID)*

Spring surface temperatures on the MID Line exhibited the same pattern as Seward and KOD Line surface temperatures in the spring (Fig. S3a) with little variation throughout and higher values in 2019 than 2018 (average difference of 0.99 °C). Fall 2019 was warmer than fall 2018, and on both summer cruises the MID Line exhibited a significant drop in temperature reaching a minimum at MID6 (2019) or MID7 (2018) followed by an increase to MID8. Overall salinity was highest in the spring. Salinity at the inshore stations reflected the influence of the Copper River and was lowest in the summer, reaching values as low as 8.70 in the furthest inshore sample during the summer 2018 cruise.

On all cruises, salinity changed most rapidly between MID1 and MID2 (Fig. S3b). In summer, however, salinity increased gradually from MID2 to MID5, while in fall salinity remained constant between MID2

and MID7 (2018) or MID5 (2019) where it increased again until Station MID8. At MID1 in spring slight decreases in salinity were measured, with values of 30.52 and 29.50 in 2018 and 2019, respectively, which were the lowest spring salinity values observed on any of the three transects. Salinity at MID10 during spring 2018 (32.39) was lower compared to the outermost stations on the Seward and KOD lines (salinity 32.6).

All seasons exhibited the same general pattern of high dAl and dMn inshore that decreased moving offshore, although spatial and interannual variability were observed. In 2018 the maxima for both metals occurred in the fall; the dAl maximum (509.7 nM) was observed in the furthest inshore sample and the dMn maximum (67.7 nM) was observed closer to MID2. During 2019 the maxima for both metals (1093.9 nM dAl and 81.0 nM dMn) were observed in the furthest inshore sample during the summer cruise (Fig. 3). The difference in dAl and dMn concentrations is similar here to that observed on the Seward Line. During summer and fall dAl values tended to be an order of magnitude higher than dMn, with the exception of the maxima observed in summer 2019 where dAl reached micromolar values. During spring when both metals were lower the average dAl:dMn ratio was 6.4. Both fall cruises also showed a slight increase in dAl and dMn around Middleton Island although summer 2019 did not.

Relationships of dAl and dMn with salinity were weakest in spring, however both metals exhibited robust linear relationships with salinity during summer and fall cruises (Fig. 4), with the slopes of these lines varying seasonally and interannually. Both metals exhibited the steepest slopes in summer 2019 and the shallowest slopes in summer 2018. Changes in dAl with salinity were greater at the MID Line compared to the Seward Line and were more varied than changes of dMn with salinity. The relationship of dAl vs. salinity was significant ($\alpha = 0.05$) during all seasons (Fig. 4), while dMn vs. salinity was not significant only in spring.

3.4. Copper River plume (Summer, 2019)

A Copper River Plume study was carried out over 5 days (7/4–7/8) during the summer 2019 cruise. It consisted of a series of transects that began at Station MID10 then moved inshore along the MID Line and sampled back and forth across the plume frontal zone between Hinchinbrook Island and Kayak Island, eventually moving southeast beyond the southern tip of Kayak Island, then turning back to the MID line and finally moving south to ~58 °N. Average daily discharge for the Copper River during this 2019 plume study was high at 8778 m^3/s (USGS). The highest daily discharge value in all of 2019 was 9798 m^3/s observed on 7/3/19, and the general peak discharge period for the year occurred from 7/2/19–7/10/19 (Fig. 5). The plume study also began during a spring tide, with a new moon on 7/2/19 and the greatest difference between high and low tides at Middleton Island occurring on 7/4/19 (NOAA tide predictions for north end of Middleton Island). The lowest temperatures (10.8 °C) were observed in proximity of Middleton Island while the highest temperatures (18.8 °C) were observed inshore in near-plume waters (data not shown). As expected, the lowest surface salinity (10.79) was observed just southwest of the Copper River delta, while the highest (32.25) was sampled in offshore waters at the end of the transect (Fig. 6a). Salinity and temperature demonstrate the inherent patchiness of surface shelf waters in the NGA. For example, a patch of warmer and fresher water off the southern tip of Kayak Island is apparent on two separate legs of the transect, and a section of the southern transect east of the MID Line exhibited fresher and warmer water than the MID Line at the same latitudes.

A concentration gradient from inshore to offshore was apparent for dAl and dMn. Dissolved Al values exceeded 1000 nM at the inshore areas near the Copper River mouth and just off the west coast of Kayak Island (Fig. 6b). In general dAl varied inversely with surface salinity as expected given high input of dAl by glacial rivers (Brown et al., 2010) (Fig. 7a). However, the highest observed surface dAl value (1394.9 nM) coincided with an intermediate salinity of 25.98 at a point off the west coast of Kayak Island in water 138.9 m deep, suggesting potential additional dAl input in this region. The range of concentrations for dMn along the transects was lower than dAl by an order of magnitude, with a maximum observed value of 128.0 nM in near plume waters, decreasing to <1 nM in offshore waters (Fig. 6c). The maximum observed dMn value was not coincident with the dAl maximum, but occurred at the sampling location closest to the mouth of the Copper River at a salinity value of 19.90.

The relationships between salinity and dissolved metals tended to be conservative in regions further away from the Copper River delta, while in shallow regions of the shelf these relationships showed non-conservative mixing, suggesting that other processes besides input of freshwater contributed to the elevated dAl and dMn values. The rapid decrease in concentration along the salinity gradient also demonstrates how efficiently dAl and dMn are removed from surface waters over the shelf and reflects some of the patchiness in the salinity/temperature fields.

Both metals showed statistically significant correlations with salinity within the plume study region ($p < 0.0001$, Fig. 7). While linear trends are apparent from salinity 21 to 32.5, many samples between salinity ~25–30 showed elevated dAl and dMn relative to salinity.

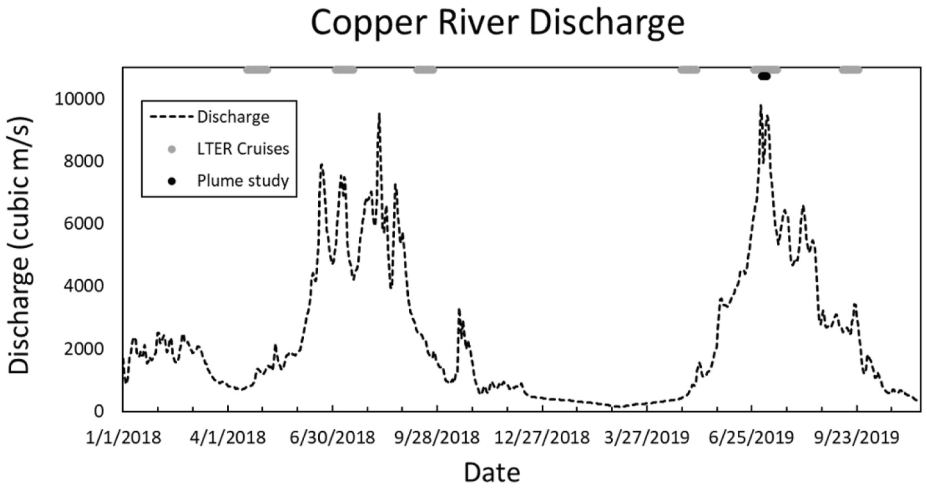

Fig. 5. Mean daily Copper River discharge (m^3/s) measured by USGS at Million Dollar Bridge. Blue markers indicate the dates of 2018 and 2019 cruises and the black marker indicates the dates of the summer 2019 plume study.

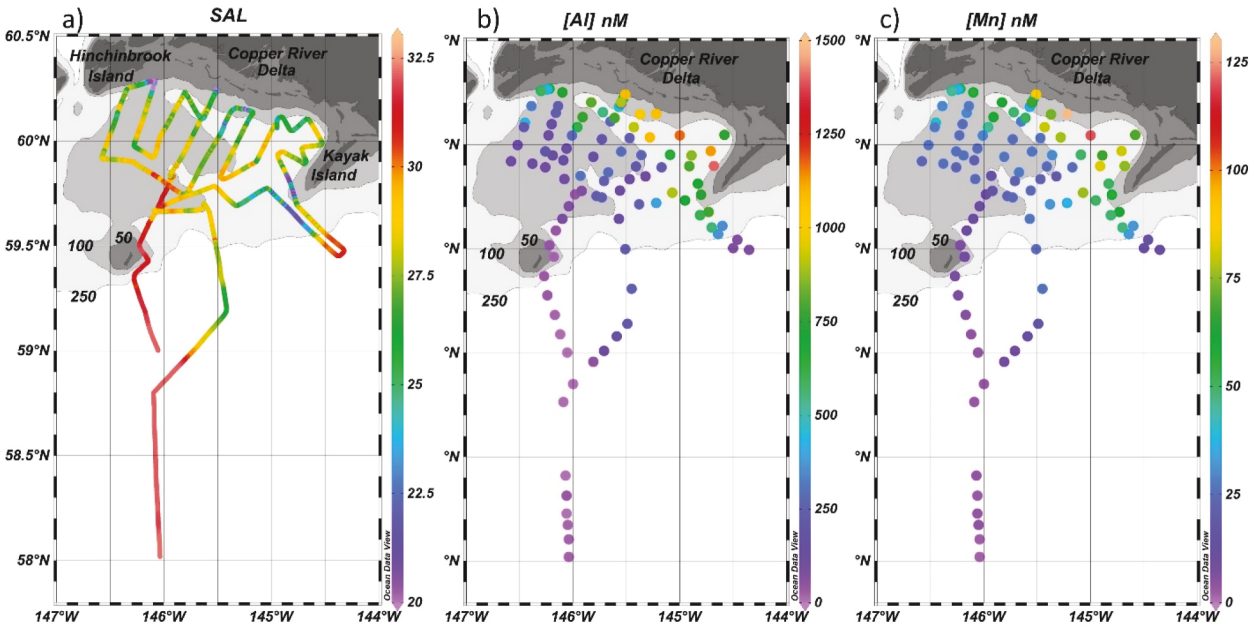

Fig. 6. a) Surface salinity (from underway data), b) dissolved Al (nM) and c) dissolved Mn (nM) during the 2019 Copper River plume study. Depth contours are marked in meters.

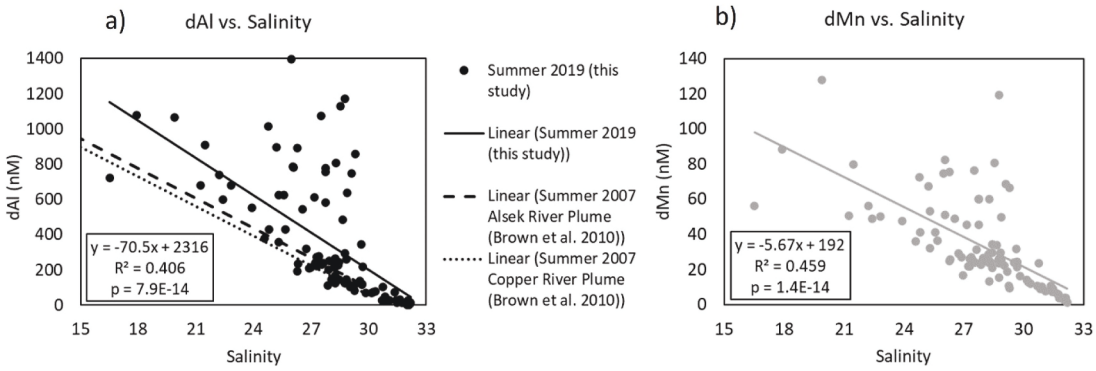

Fig. 7. a) Dissolved Al and b) dMn as functions of salinity for the summer 2019 Copper River plume study. Also included in (a) are the trendlines for summer 2007 plume studies in the Alsek River (dashed line) and the Copper River (dotted line) presented in (2010).

3.5. Residence times

Residence times were estimated for surface dAl and dMn over the shelf in the area around the inner MID Line and Copper River outflow (Table 4). In all seasons the estimated residence time for dAl was lower than that for dMn and in both years it was lower in summer than fall, yielding an overall average of 31 days for dAl and 42 days for dMn. The residence times calculated for both metals in 2018 are more than double those calculated for the same seasons in 2019. For summer, this is mostly due to differences in Copper River outflow between the two years while in fall this difference is mostly due to much larger dAl and dMn reservoirs in 2018 (section 2.4).

3.6. Depth profiles (Spring 2018 and Summer 2019)

Vertical profiles were collected at six stations (Fig. 2). Temperature and salinity profiles for Station KOD5 indicate a relatively well-mixed water column in spring 2018 compared to summer 2019. The profiles for light transmission indicate a gradual increase in particles with depth during spring 2018. During summer 2019, temperature, salinity and beam transmission indicate a surface mixed layer down to 20 m that transitioned to a well-mixed deeper layer below 30 m (Fig. 8a). During both seasons, somewhat greater vertical variability was observed for dAl than for dMn (Fig. 8b and c). During spring 2018 both metals tended to increase with depth and had subsurface maxima at 40 m (20.6 nM dAl; 6.2 nM dMn). In summer 2019, dMn also tended to increase with depth, with a minimum (4.4 nM) at the surface and a subsurface maximum at 50 m (6.8 nM). In contrast, dAl appeared to decrease with depth in summer 2019. The surface and 50 m values (summer 2019) for dAl were lost during processing and could not be quantified.

Temperature and salinity at GAK1 indicated a colder water column in the upper ~200 m in spring 2018 compared to summer 2019, and much fresher water in the upper 15 m during summer (data not shown). Deeper water (below 200 m) at this station had similar T and S characteristics during both seasons. A lower particle load over the entire water column was observed in spring compared to summer, with summer 2019 exhibiting a near-surface particle maximum at 18 m from biological particles and a bottom particle maximum from resuspended sediment (Fig. 9). In contrast, spring 2018 exhibited a less pronounced particle maximum at depth and no observable maximum at the surface. In general dAl tended to be present in greater concentrations than dMn at GAK1. Surface inputs for dAl and dMn were particularly apparent in

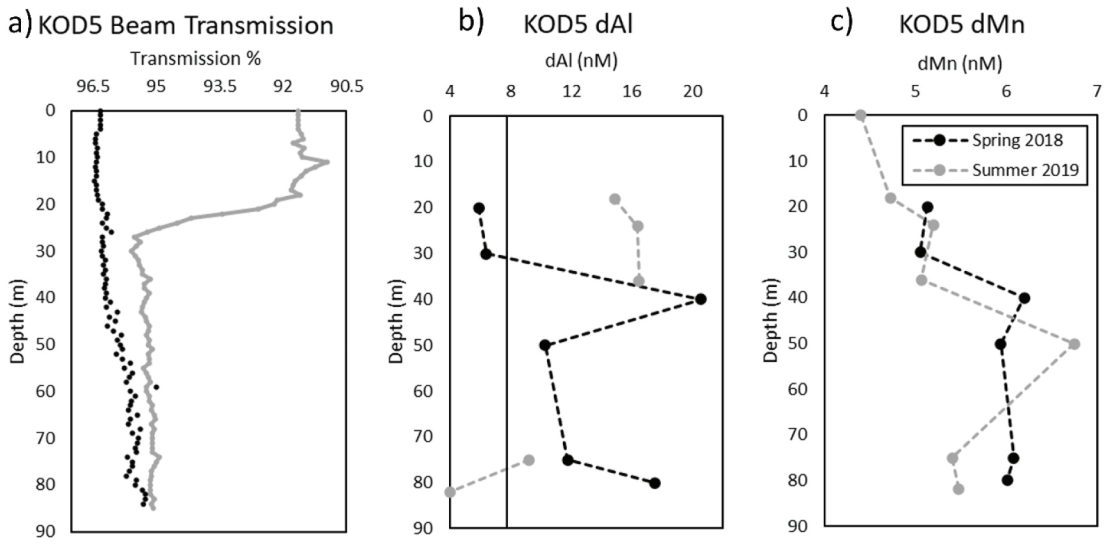

Fig. 8. a) Transmissivity, b) dAl (incl. LOD), and c) dMn values for KOD5 from CTD casts on 4/19/18 and 7/15/19. The bottom depth at KOD5 is 87 m.

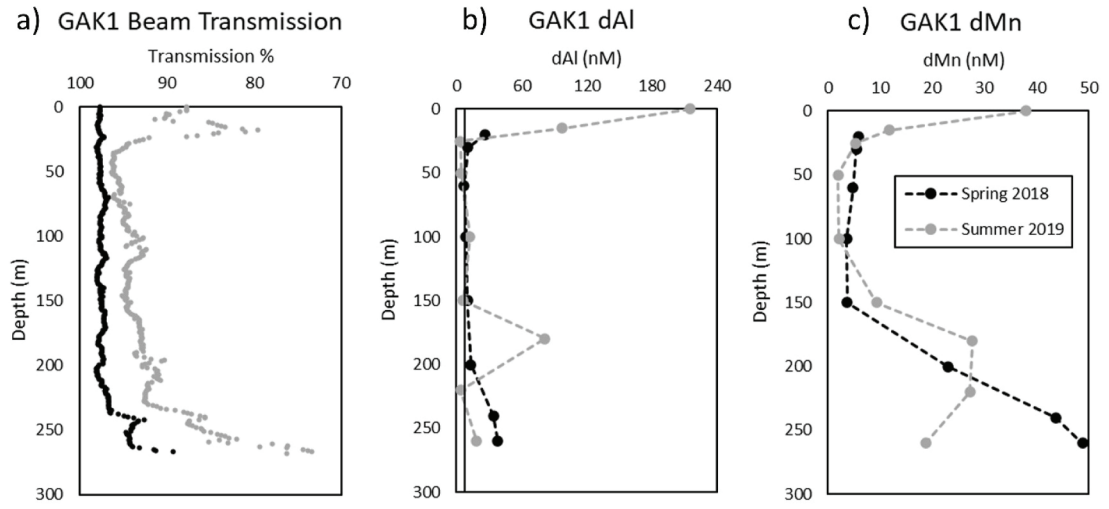

Fig. 9. a) Transmissivity, b), dAl, and c) dMn values for GAK1 from CTD casts on 5/4/18 and 6/29/19. The bottom depth at GAK1 is 270 m.

summer 2019 with surface maxima for both metals (as high as 214.5 nM for dAl and 38.0 nM for dMn) that decreased rapidly with depth (Fig. 9b and c). During spring 2018, a sedimentary source for both metals was apparent in enhanced metal concentrations (38.0 nM dAl, 48.8 nM dMn) below 200 m that coincided with the decrease in transmissivity. This systematic increase in dAl and dMn with depth in the deeper layers of the water column was not apparent in summer 2019, although the decrease in light transmission was more pronounced and subsurface maxima were observed at 180 m for both dAl (81.3 nM) and dMn (27.7 nM). Vertical distributions at GAK1 at intermediate depths (30–150 m) fell within 3.4–12.0 nM for dAl and 1.9–9.3 nM for dMn during both seasons.

While the temperature profiles at GAK5 closely mirror those at GAK1 during both seasons, the decrease in surface salinity in summer 2019 at GAK5 was much less pronounced (data not shown). This shallower station exhibited seasonal differences in its deeper waters with summer 2019 carrying saltier offshore waters below 100 m. An increase in suspended particles was observed at 30 m during spring 2018 and at 15 m during summer 2019 at this station. Similar to GAK1, maxima in suspended particles in bottom waters were also observed at GAK5 during both seasons. At GAK5 dAl concentrations were greater than dMn concentrations during both seasons, and as expected surface maxima for both metals were lower than at GAK1. In general, the surface maxima were more pronounced for dMn in summer 2019 compared to spring 2018, while surface waters exhibited similar dAl (~8 nM) during both seasons (Fig. 10). At intermediate depths (20–75 m), lower concentrations of both metals were observed during summer 2019 as compared to 2018. In general, metal concentrations tended to increase below 100 m during both seasons and during summer 2019, subsurface changes in dAl mirrored changes the transmissivity data that showed two regions with increased suspended particles at 120 m and 167 m (Fig. 10).

Station MID2 is an inner-shelf station, and similar to GAK1 this location exhibited much lower surface salinity in summer 2019 (27.2) relative to spring 2018 (32.0). Here, warmer waters were observed in summer 2019 throughout the entire water column compared to spring 2018, and deeper waters (below 75 m) were fresher in the spring profile (data not shown). Also similar to GAK1, beam transmission throughout the water column was reduced during summer 2019 compared to spring 2018. A signal from resuspended particles was apparent from the bottom up to ~100 m depth during both seasons, and the upper water column (surface to ~40 m depth) exhibited more structure in beam transmission during summer 2019 than in spring 2018. During spring 2018 dAl and

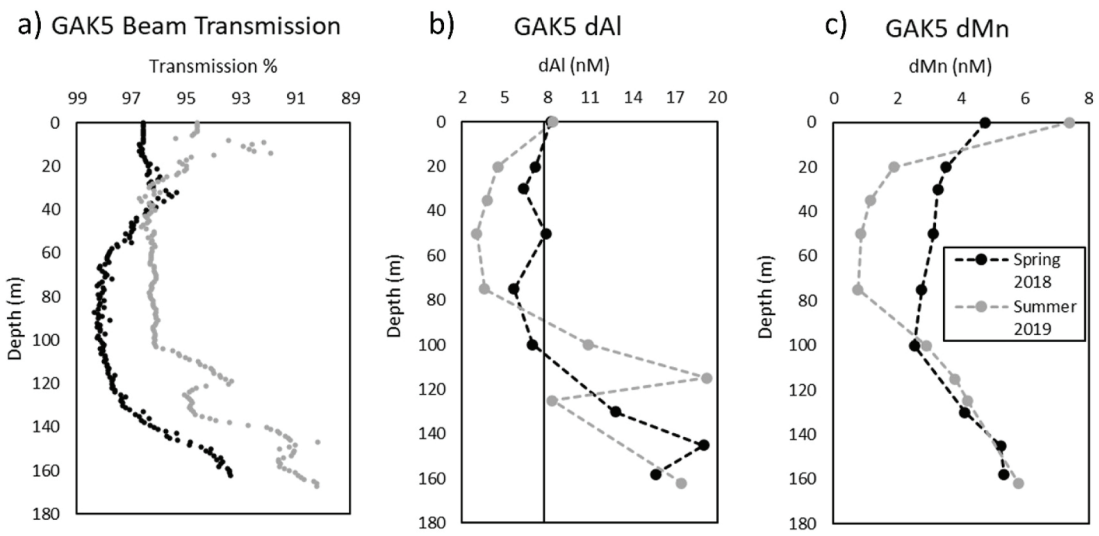

Fig. 10. a) Transmissivity, b) dAl, and c) dMn values for GAK5 from CTD casts on 5/3/18 and 7/13/19. The bottom depth at GAK5 is 167 m.

dMn values were lower than in summer 2019 throughout the water column (Fig. 11b and c). Also, dMn during both seasons and dAl during spring 2018 increased in the bottom two samples tracking the decrease in transmissivity at the bottom of the water column. However, dAl in summer 2019 exhibited greater concentrations at mid-depths (50–75 m) than at the bottom two samples.

The temperature profiles observed at MID5 followed the same broad pattern as other shelf stations, with colder waters and less variability in spring 2018 compared to summer 2019. Surface temperatures during summer 2019 were cooler than those at GAK5, but warmer than surface waters at KOD5. The observed salinity values at MID5 were fresher than those observed at GAK5 throughout the water column, and the salinity profile in spring 2018 indicated stratification in the upper 30 m which was not apparent in the temperature data (data not shown). At this station, lower beam transmission was also observed in summer 2019 compared to spring 2018, with the exception of the region between ~25 and 50 m. The difference in surface dAl between MID2 and MID5 in summer 2019 (221.0 nM vs. 52.8 nM) emphasizes the rapid loss of dAl moving offshore. Similar to MID2 (and other shelf stations) the impact of fresh water on surface metal concentrations is less pronounced for dMn, with MID5 exhibiting no enhancement in dMn at the surface between spring and summer. In both seasons dMn concentrations were lower at mid-depths (20–50 m), indicating surface and bottom inputs. A bottom input for dAl was not pronounced here. (Fig. 12). Samples for dAl for spring 2018 are not included as the samples sat too long between pre-concentration and analysis and the dAl data were unusable.

Prince William Sound is impacted by several surrounding glaciers and includes regions with depths greater than the shelf stations along the three transects. Evidence of a stratified water column was apparent at PWS2 from the temperature, salinity, and beam transmission in spring 2018 (Fig. 13a). Surface temperatures at PWS2 during spring 2018 were comparable to those at GAK1, although surface salinity was fresher at GAK1. Similar to other stations, surface waters at PWS2 were warmer and fresher during summer 2019. More seasonal variability in temperature and salinity was observed between 100 and 500 m than below 500 m. Reduction in beam transmission was more pronounced at the surface during summer 2019, but the reduction in beam transmission at the bottom was greater during spring 2018. Beam transmission was also reduced from 250 to 650 m during summer 2019 compared to spring 2018. Vertical distributions for dAl and dMn at PWS2 generally exhibited greater concentrations during summer 2019 than during spring 2018 (Fig. 13b and c), particularly below 100 m. There was a surface input signal for both metals in both seasons but below 20 m dAl exhibited more variability than dMn. In spring 2018 dMn gradually

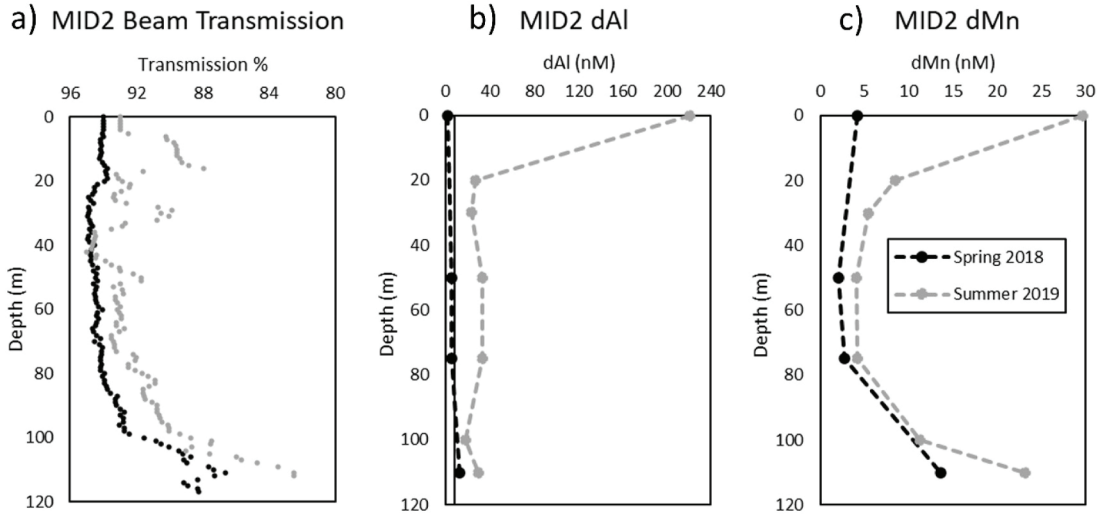

Fig. 11. a) Transmissivity, b) dAl, and c) dMn values for MID2 from CTD casts on 4/26/18 and 7/1/19. The bottom depth at MID2 is 118 m.

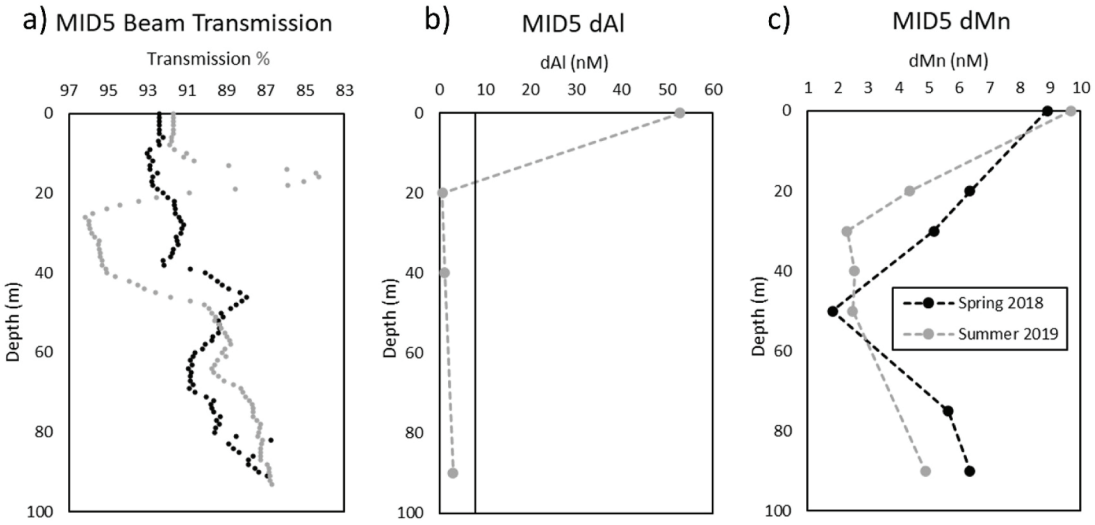

Fig. 12. a) Transmissivity, b) dAl, and c) dMn values for MID5 from CTD casts on 4/27/18 and 7/2/19. The bottom depth at MID5 is 95 m.

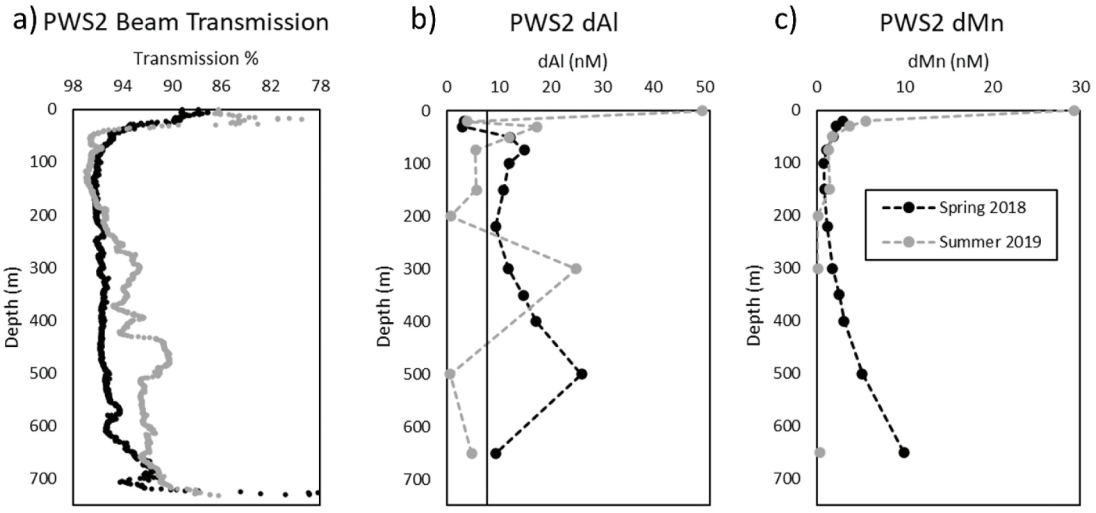

Fig. 13. a) Transmissivity, b) dAl, and c) dMn values for PWS2 from CTD casts on 4/23/18 and 6/30/19. The bottom depth at PWS2 is 728 m.

decreased from the surface to a minimum (0.8 nM) at 100 m, and then increased gradually to a maximum of 9.9 nM at the bottom of the water column. This pattern mirrors changes in the transmissivity data (Fig. 13a). In summer 2019 dMn decreased with depth to subnanomolar concentrations below 200 m (0.06–0.28 nM) with the lowest value at 500 m, which could not be quantified accurately with our methods. In spring 2018 dAl had subsurface minima at 220 m (9.3 nM) and 650 m (9.5 nM), and subsurface maxima at 75 m (14.9 nM) and 500 m (26.0 nM). Similarly, in summer 2019 dAl exhibited two subsurface maxima but at different depths; 30 m (17.4 nM) and 300 m (25.1 nM). In spring 2018 a decrease in dAl at 650 m coincided with the area of increased beam transmission.

4. Discussion

4.1. Freshwater influences on surface dAl and dMn

Surface waters on the Middleton, Seward, and Kodiak transects are impacted to various degrees by riverine/glacial inputs based on their proximity to large fresh water sources such as the Copper River. Due to its proximity to the Copper River, the largest single point source of fresh water in the NGA, the MID Line tended to be the freshest, particularly in summer/fall. The KOD Line was the most oceanic in character, particularly during spring, whilethe Seward Line exhibited intermediate characteristics. The degree of freshwater entrainment was reflected in surface salinity values and was generally the main influence on concentrations of surface dAl and dMn along the shelf, with dMn exhibiting in general a more robust linear relationship with salinity than dAl. The overall decrease in inner shelf dAl and dMn from the MID Line to the KOD Line emphasizes the importance of the Copper River as a point source for these metals. The lack of other large point sources west of the Copper River as well as the particle-reactive nature of both metals contributed to the observed decrease of dAl and dMn along the ACC. The efficiency of metal scavenging in these advective coastal waters, where biogenic and lithogenic particles tend to be the highest, is exemplified by the changing relationship of dAl and dMn with salinity along the path of the ACC, with mixing lines becoming less steep to the west. Steep inshore/offshore gradients in both metals also highlight the key role of the ACC in keeping freshwater with higher dissolved metals closely constrained to the nearshore. Regardless of how high the dAl and dMn were inshore, their concentrations in the mid to outer shelf decreased to similar ranges in every season (~1–12 nM dAl and <1–4 nM dMn) (Fig. 3) with the exception of fall MID transects when low-salinity, high dissolved metal waters extended further offshore. The lowest dAl (0.9

nM, salinity 32.29 nM) and dMn (0.4 nM, salinity 32.54) values determined during this study were in offshore waters. These do not reflect the low trace metal oceanic endmember with salinity in the range of 32.6, as the detection limit of our pre-concentration method was higher than the low dAl value measured previously in the NGA (0.08 nM at salinity 32.45 on the Seward Line) (Brown et al., 2010).

Given that fresh water is the main source of both metals in this region, a primary external factor affecting seasonal patterns in surface dAl and dMn is glacial melt. Glaciers encompass an area 72,000 km^2 in the GOA watershed (Beamer et al., 2016) and peak melt season tends to occur in late summer/early autumn, during which period runoff has been shown to double compared to the rest of the year (Royer 1981; Hill et al., 2015; Beamer et al., 2016) as was the case during our study years (Fig. 5). While seasonal patterns in surface dAl and dMn in our study region were mainly a result of glacial melt cycles, seasonality in trace metal distributions in areas without glacial influence may look different. In a study of the Mississippi River, dMn was lowest during summer, increasing rapidly in late fall (Oct Nov) and then decreasing throughout spring (Shiller 1997). This pattern is thought to be due to reducing conditions within the river basin during winter that reduce Mn oxides to dMn. In northern San Francisco Bay, dissolved Mn was observed to decrease in winter and spring due to adsorption, likely onto both inorganic and biogenic particles, while in southern waters dMn was highest in winter and summer due to reductive dissolution in the sediments (Roitz et al., 2002). A study of temporal Mn (and Cd) variability in the Hudson River estuary found a third type of seasonality, in which dMn actually decreased with higher river flow (Yang and Sanudo-Wilhelmy 1998).

The influence of seasonal patterns of riverine input on surface trace metal distributions were clearest on the Seward and Middleton Lines that showed the lowest dAl and dMn concentrations in spring when glacial melt was minimal. The KOD Line, which is the least influenced by freshwater input of the three transects, also contained higher surface dAl and dMn values during the fall, but had comparable dAl and dMn values in spring 2019 and summer 2018 with the lowest values observed for both metals occurring in summer 2019. All three transects, however, generally had the highest metal concentrations in fall 2018. Interannual differences in Copper River discharge, as integrated outflow from May 30 Sept 11 (the start date of the fall cruise both years) was comparable in 2018 and 2019 (6.88 10^{12} m^3 vs. 6.60 10^{12} m^3, respectively) (USGS). Given the advective nature of the GOA shelf system, a direct correlation between integrated river discharge values and surface dAl and dMn values at different locations along the ACC was not possible to determine.

River discharge is likely not the only factor affecting interannual dAl and dMn fluctuations within a given season along ACC waters. Storms prior to sampling could break surface stratification and dilute dAl and dMn concentrations by mixing surface waters with subsurface waters (down to ~100 m in winter/spring or ~40 m in summer/fall) lower in dissolved metal values (Fig. 3). For example, the lower values (and shallower mixing lines) observed during fall 2019 compared to fall 2018 (Figs. 3 and 4) could be explained by storm mixing events, given that the fall 2019 field season was heavily impacted by storms, while the fall 2018 field season had calm conditions prior to and during sampling.

Along the Seward Line, inner shelf (within the ACC) metal concentrations were highest in fall in both years followed by summer (Fig. 3c and d), whereas along the MID Line inshore values for both metals were within the same range during summer and fall occupations (Fig. 3e and f). This suggests that for inshore MID Line waters, which are in close proximity to the Copper River outflow, daily river discharge influences the concentration of dAl and dMn within fresh river plumes near the outflow. In contrast, on the Seward Line, high dAl and dMn values sampled within the ACC better reflect integrated freshwater discharge (including outflow from Prince William Sound). This difference in seasonal patterns between the two transects reflects the particle reactive nature of both dAl and dMn, leading to overall loss of both metals as surface waters mix and age along the coast from the inshore MID Line to the inshore Seward Line.

Plots of dMn as a function of dAl (Fig. 14) highlight the tight correlation between these two metals within the Copper River plume, and more broadly in surface fresh waters of the inner shelf. This correlation became much less robust in regions least impacted by freshwater input. On the KOD Line the lack of correlation (p 0.1) between dAl and dMn during spring and summer suggests that at these times processes other than freshwater input determined surface dAl and dMn distributions. Similarly, along the Seward Line, there was low correlation (R^2 of 0.215) between dMn and dAl during spring, when the Seward Line was least impacted by freshwater. At a significance level of 0.05 this relationship was still statistically significant, although this p-value (0.0016) was the highest observed on the Seward Line by 2 orders of magnitude. In general, decoupling between the surface dMn and dAl concentrations could serve to pinpoint regions over the shelf where processes other than river input may be impacting surface waters at a given time. Differences in slope, both between the three cruise lines and between different seasons on each line, also indicate controls on dAl and dMn distributions by other processes. For example, on the MID Line, slopes were steeper in spring 2019 than both summer occupations (Fig. 14c) suggesting increased removal of dAl, increased input of dMn in summer, or perhaps some combination of these processes. Higher dMn relative to dAl in spring vs. summer was apparent throughout the water column in inshore waters based on the vertical profiles obtained at MID2, as the dMn/dAl slope was ~10x higher in spring 2018 than in summer 2019 (data not shown). Potential mechanisms for dMn input throughout the water column include photoreduction of particulate Mn (Sunda and Huntsman 1988) in surface waters or Mn respiration in sediments (Froelich et al., 1979). Winter mixing could carry either signal throughout the water column. Intense particle scavenging, which disproportionately affects dAl (Bruland and Lohan 2003) could also contribute to the observed dMn/dAl ratios.

4.2. *Influence of bathymetry on dAl and dMn*

Bathymetric features of the NGA shelf are highly irregular, and our study area is characterized by a series of banks and troughs (Gibson 1960; Zimmermann and Prescott 2015) that are unevenly distributed and contribute to the complexity of the NGA environment. The KOD Line crosses the northeast side of North Albatross Bank, which is separated from Portlock Bank by the Stevenson Trough. The MID Line is also positioned across a large bank (Tar Bank) and the shoals surrounding Middleton Island before making a turn southeast across the slope. The plume study in summer 2019 also covered part of Kayak Trough and shallow regions near the Copper River outflow. The Seward Line bathymetry is yet more complex, crossing a relict moraine on its trajectory towards Amatuli Trough before reaching the slope.

Higher chlorophyll values relative to surrounding waters have been observed over shallow banks such as Albatross Bank due to enhanced vertical mixing that brings macronutrients from subsurface waters up to the surface (Cheng et al., 2012). Vertical mixing over the shallowest region of the bank could also provide elevated trace metals to surface waters. This process can help explain the enhanced values of dMn (Fig. 15) that we observed over the section of the KOD Line that crosses North Albatross Bank, which were more pronounced in spring 2019. Dissolved Al over the bank exhibited some elevated values, but the pattern was less distinct (data not shown). During spring 2019 dMn was almost twice as elevated over Albatross Bank (maximum of 6.9 nM) compared to its concentration in the furthest inshore sample (3.6 nM). In general, hydrographic sections for the KOD Line (Fig. S4) indicate less stratification throughout the water column over Albatross Bank in spring compared to fall, which suggests that the signal of subsurface metals from winter mixing is still influencing surface waters. This is supported by the vertical profiles of dMn at Station KOD5 (Fig. 8).

It is reasonable that the enhancement in concentration in the

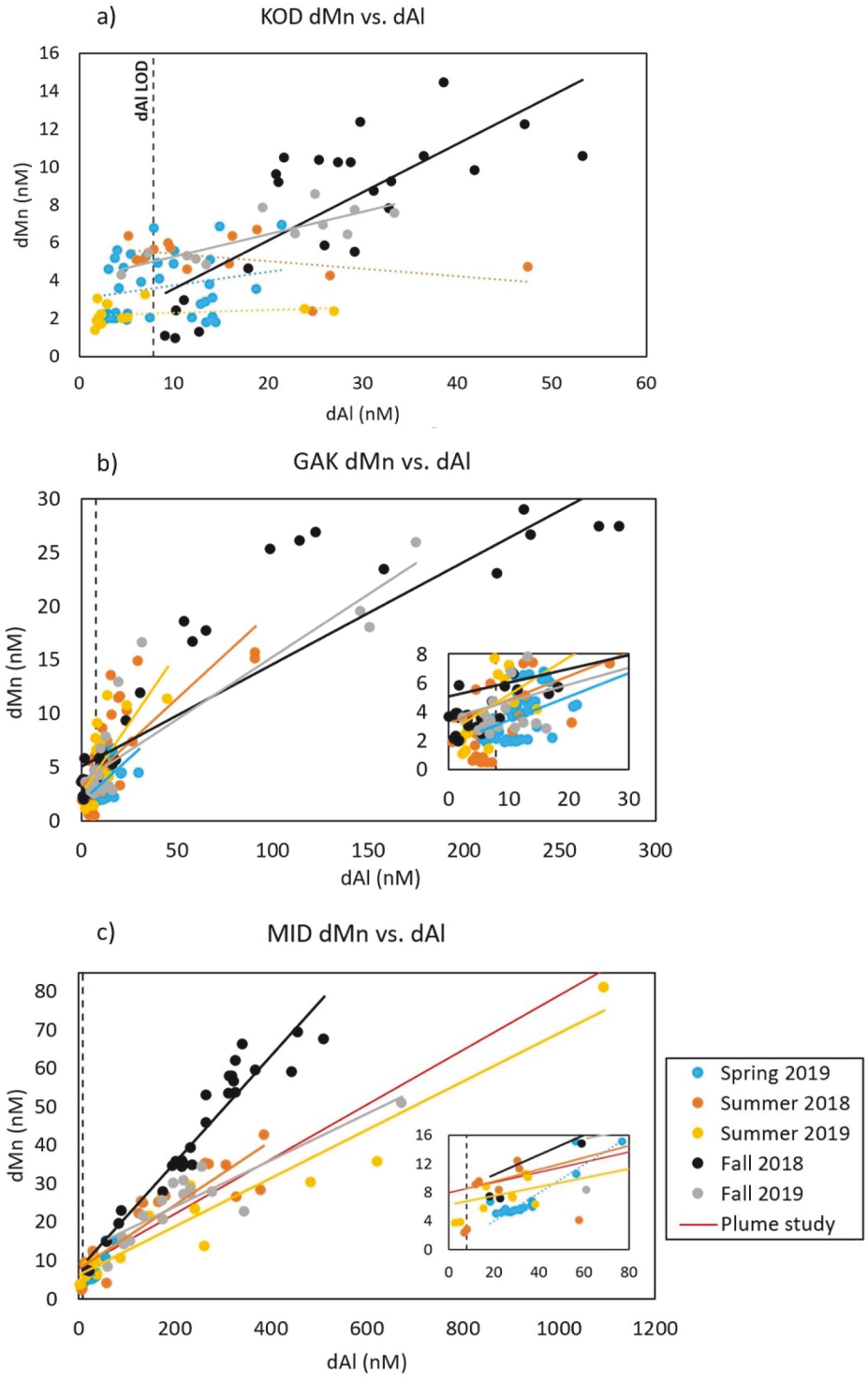

Fig. 14. Dissolved Mn as a function of dAl along the a) KOD, b) Seward, and c) MID Lines for all 2018 and 2019 cruises except for spring 2018. The insert in (b) ranging from 0 to 8 nM dMn and 0–30 nM dAl highlights samples with low dAl and dMn values. In (c) a trendline for plume study data (summer 2019) is also included. All data are shown, and the line in (a), in the inserts of (b) and (c), and in (c) at 7.8 nM dAl show the dAl LOD. Solid trendlines indicate relationships that are statistically significant ($\alpha = 0.05$) and dotted trendlines indicate those that are not.

productive waters over Albatross Bank is clearer for dMn than for dAl in spring given the biogeochemistry of Mn in seawater. Particulate Mn in the form of Mn oxides (Mn(III) and Mn(IV)) may be reduced in sediments to dMn (Mn^{2+}) via anaerobic respiration, as Mn oxides are efficient oxidants utilized in suboxic/anoxic environments (Froelich et al., 1979). This reductive dissolution of Mn oxides in the sediment can provide an input of dMn to the water column that can then be mixed to the surface in shallow areas such as banks during mixing events. The enhanced production over Albatross Bank throughout the growing season (Waite and Mueter 2013) likely results in enhanced organic matter input to the sediment leading to enhanced respiration and oxygen utilization in surface sediment, creating an environment where reductive dissolution of Mn oxides could take place (e.g., Rutgers Van Der Loeff et al., 1990). This process occurs for iron as well, so if these enhanced dMn values over North Albatross Bank in spring are indicative of winter anaerobic respiration in the sediments, dFe might also be enhanced. In addition, there would be implications for nitrogen cycling in this region as metals are less efficient electron acceptors than nitrate, so their utilization for respiration in a given area suggests denitrification has taken place and the available nitrate in pore waters has already been depleted

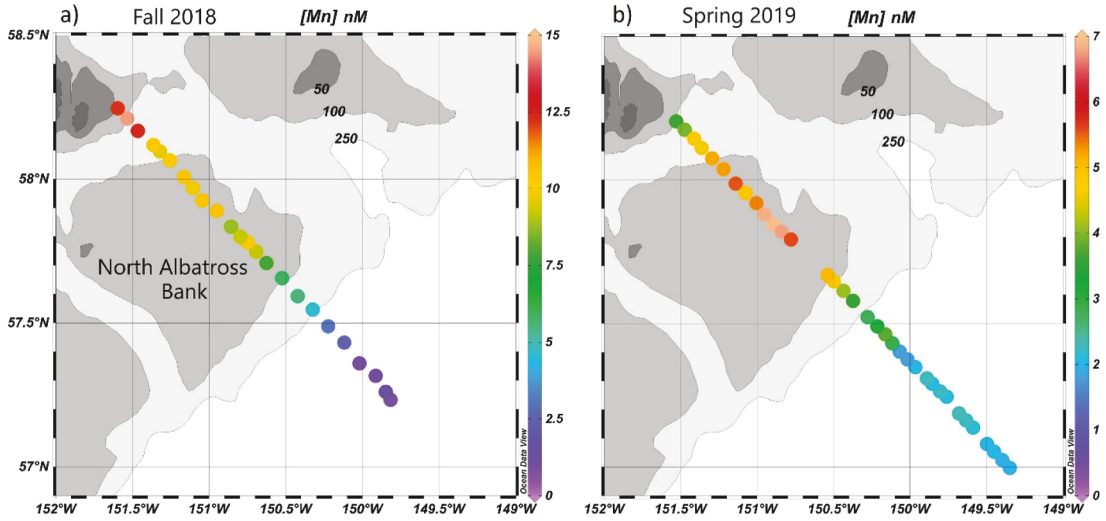

Fig. 15. Map with superimposed surface dMn values along the KOD Line during a) fall 2018 and b) spring 2019. Depth contours are marked in meters.

(Froelich et al., 1979).

Alternatively (or concomitantly), enhanced dMn (and dFe) concentrations at the surface could result from photoreduction of suspended particulate Mn oxides (e.g., Sunda and Huntsman 1994) brought to the surface during mixing events, such as storms or enhanced tidal mixing. Indeed, greater influence of tidal mixing is expected in spring compared to fall based on changes in water column stratification, and tidal amplitude may also play a role. In spring 2019 when the dMn increase over Albatross Bank was clearly observed (Fig. 15b) the KOD Line was sampled during spring tide condition (NOAA tide data for Port of Kodiak), whereas in fall 2018 the KOD Line was sampled during neap tide conditions (NOAA tide data for Port of Kodiak). It is also important to note here that the photodissolution process affects particulate phases of Fe as well as Mn.

Subsurface input from Tar Bank along the MID Line is harder to discern, given the influence of the Copper River on surface dMn concentrations. However, focusing on spring data, when river discharge is low, surface dMn concentrations over Tar Bank (~5.5–7 nM; salinity 31.8–32.2) were similar to those over Albatross Bank (~5–7 nM; salinity 32.3–32.4) at comparable salinities. The vertical profiles of dMn for MID2 and MID5 exhibited little variability below 20 m in spring and summer (Figs. 11 and 12), suggesting a potential input of dMn from the subsurface not just in spring. Similar to Albatross Bank, tidal mixing is likely an important mixing mechanism over Tar Bank supplying dissolved metals and nutrients to surface waters. Tides have also been shown to affect dMn values in river plumes. Aguilar-Islas and Bruland (2006) observed that dMn in near-field Columbia River plumes varied widely with tidal amplitude. Much higher concentrations of dMn were found when plumes were sampled during a spring tides than when sampled during neap tides, and difference was attributed to enhanced suspended sediment loads during spring tides and photoreduction of Mn oxides.

4.3. Residence times

To determine the seasonal influence of Copper River outflow, residence times for surface dAl and dMn were estimated for the two seasons of greatest river discharge as described in section 3.5. The estimated residence times of both metals were on the order of days to tens of days for the two seasons when river discharge is pronounced, with fall having longer residence times for both metals, and dMn having longer residence times than dAl (Table 4). This is reasonable as Al is a highly particle reactive lithogenic metal (e.g., Hydes 1979), while Mn, although required by biology is less particle reactive, and concentrations of dMn in surface waters can be augmented via photoreduction (Sunda and Huntsman 1994). Our estimates for the residence times of dAl are in line with the value calculated by Brown et al. (2010) (~10-days) for a broader region of the NGA surface waters from data obtained during August 2007.

4.4. Plume study

The tight coupling observed between surface dAl and dMn in our plume study indicate that both metals generally came from the same source, i.e., river discharge (Fig. 16). In near-field plume waters dAl was approximately an order of magnitude more concentrated than dMn. The values of dAl we observed in this region are in line with those presented in Brown et al., (2010) (from August 2007). The range of dAl values they observed near the Copper River outflow (salinity 19.2–28) was 116–620 nM. Also, near the Alsek River outflow they reported dAl values as high as 1150 nM in fresh (salinity 7.44) surface waters. Similarly, we observed extremely high dAl values ranging from 220.7 to 1395 nM within low salinity waters (16.51–29.68) of the Copper River plume. While the relationship we observed between dAl and salinity during summer 2019 was statistically significant (Fig. 7a, $\alpha = 0.05$; $p = 7.9E\text{-}14$) the linearity was much lower than that observed in 2007, due to elevated dAl data between salinity 25–30 (likely a result of continued desorption from particles in the high sediment load carried by the glacially-fed Copper River). The steeper slope and higher zero-salinity endmember in 2019, contributed to our calculated dAl residence time being shorter than that reported in Brown et al., (2010) (5 days vs. 10 days; Table 4). Many of our samples with salinity 25–30 and dAl <400 nM match well with the values observed in 2007. The overall higher dAl concentrations we observed in July 2019 compared to 2007 could be explained by differences in Copper River outflow at the time of sampling – mean discharge was 3945 m^3/s from 8/25/07–8/27/07 while from 7/4/19–7/6/19 it was 8467 m^3/s.

The higher river discharge is likely accompanied by greater suspended loads of glacial flour, and although we did not measure total suspended solids (TSS) in our samples, Brown et al. (2010) found a weak correlation in dAl and TSS within Copper River plume waters. The very high dAl values we measured during summer and fall confirm the observation in Brown et al. (2010) that coastal GOA waters are generally higher in dAl (by one to two orders of magnitude) than other coastal shelf areas impacted by rivers such as the Columbia River region off the Oregon coast (Brown and Bruland 2009) and the Yangtze River region in the East China Sea (Ren et al., 2006). In contrast, high dMn values in the Copper River plume were approximately half as high (~130 nM) as the

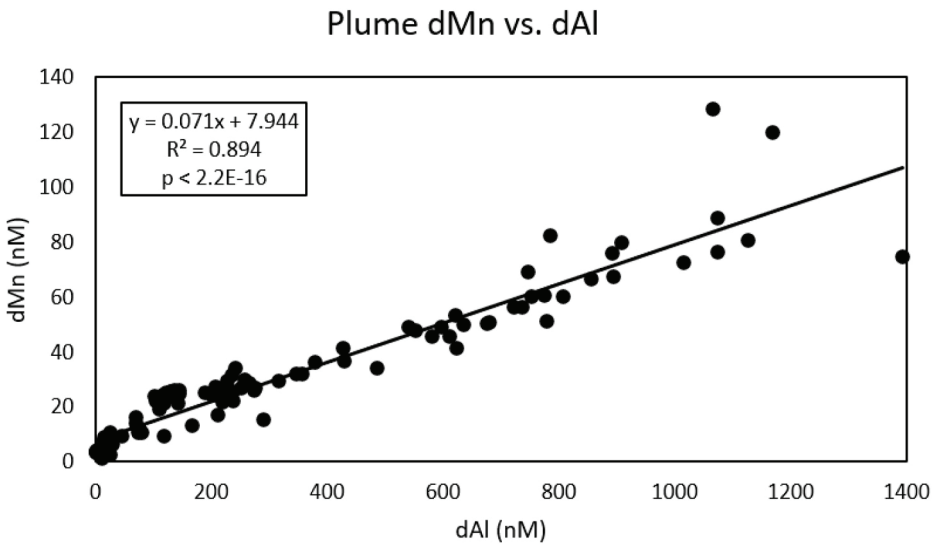

Fig. 16. Dissolved Mn as a function of dAl for the Copper River plume study (summer 2019).

highest concentrations measured in the Columbia River plume (~240 nM) at comparable salinities (Aguilar-Islas and Bruland 2006). The type of rock eroded along with the balance between competing dissolution/scavenging processes in waters with high suspended particulate loads allows for observed variations in the riverine delivery of dissolved metals to coastal waters.

For example, zero-salinity endmembers estimated for the Copper River are markedly different from estimates for other coastal areas influenced by river input. The endmember dAl values calculated for the Copper River from our MID Line data range from 820 nM in summer 2018–2520 nM in summer 2019 (the value for summer 2018 may be an underestimate, resulting from generally low dAl values associated with sampling during neap tide conditions). The dAl concentration calculated in Brown et al. (2010) for the Copper River, 1740 nM, falls within this range, which is much higher than estimates from other regions. Plots of dAl vs. salinity in the previously mentioned Columbia River and Yangtze River plume studies led to zero-salinity endmember values of ~85 nM and 220 nM dAl, respectively (Brown and Bruland 2009; Ren et al., 2006). This suggests that the lower dAl values observed in these regions at comparable (or lower) salinities to our plume study directly resulted from lower dAl in the rivers themselves. The apparently high dAl content in the Copper River is likely due to the high load of glacial flour carried in this river, which consists of aluminosilicate materials and results from intense physical weathering of nearby glaciers (Spotila et al., 2004). This is supported by a similar zero-salinity endmember dAl estimate (1792 nM) for the Alsek River, another glacially-fed river in Alaska (Brown et al., 2010).

4.5. *Dissolved Al and Mn as tracers of the dFe input into the NGA*

The distributions of dAl and dMn in plume waters have the potential to provide insight into the seasonality in the freshwater endmember for dFe. This is due to the quasi-conservative behavior of dAl and dMn relative to salinity in plume waters compared to that of dFe, which does not exhibit a lienar relationship with salinity in low salinity (9–27) waters. All three metals are lithogenic elements (Al constitutes 8.23%, Fe 5.63% of continental crust, and Mn is found at 716 ppm by weight (Taylor, 1964)) and are particle reactive to differing degrees, with dAl and dFe being more easily scavenged by particles than dMn (Landing and Bruland 1987; Bruland and Lohan 2003). Compared to Al, the biogeochemistry of Mn has more similarities to that of Fe as they are both micronutrients that can also undergo reductive dissolution via anaerobic respiration in sediments (Froelich et al., 1979) or photoreduction of particles in surface waters (Sunda and Huntsman 1994). However, cellular requirements for Fe are higher than those for Mn (Twining and Baines 2013). Another difference is that dFe is >99% bound by organic ligands in seawater (e.g., Rue and Bruland 1995), while neither dAl nor dMn is bound by organic ligands to a significant extent (Jones et al., 2020; Orians and Bruland, 1986).

Iron is an essential micronutrient used by phytoplankton for processes such as photosynthesis and nitrate acquisition, and is regarded as the limiting nutrient in HNLC waters such as those in the offshore NGA. Over the NGA shelf during spring, dFe concentrations can be deficient relative to available nitrate when compared to diatom requirements (Aguilar-Islas et al., 2016). Fe-binding organic ligands control dFe concentrations (e.g., Buck et al., 2007) in seawater by forming complexes with Fe, such that these naturally-occurring ligands increase the amount of Fe that can exist in the dissolved form in seawater. Thus, Fe-binding organic ligand concentrations can set an upper limit on dFe concentrations, although inorganic colloidal Fe can also contribute to enhanced dFe concentrations in coastal waters (Wu and Luther 1994). A small dataset of Fe-binding organic ligands in the NGA (Aguilar-Islas et al., 2016) shows Fe-binding organic ligand concentrations are always in excess relative to dFe in spring and summer. Consequently, the seasonal freshwater input of dFe into the coastal NGA can be obscured by high biological uptake coupled with dependence on Fe-binding organic ligand availability.

Plots of dFe as a function of dAl and dMn from our Copper River plume study illustrate the potential control organic Fe-binding ligands exerts over dFe concentrations (Fig. 17). In surface waters during the plume study, dAl and dMn were tightly coupled to salinity and each other in surface waters collected during the plume study (Figs. 7 and 16), while dFe was not (data not shown). The concentration of dFe was decoupled from these metals, particularly at higher dAl (>~200 nM) and dMn (>~20 nM) concentrations, where dFe values were capped ~6 nM, with most dFe values in the 2–3 nM range. This decoupling suggests either intense biological uptake of dFe in fresher plume waters, or low concentrations of available Fe-binding organic ligands that cap dFe concentrations in these surface waters. Lippiatt et al. (2010) also found that dFe did not surpass concentrations of ~2.5 nM in coastal waters near the Copper River plume at salinity values comparable to those sampled during our plume study (minimum salinity of 16.5 in 2019 vs. ~19 in 2007).

To further visualize how dFe varied relative to dMn, the ratio of dFe: dMn was plotted as a function of dMn (Fig. 18), separating offshore waters (salinity >31.75) from plume waters. This plot highlights where

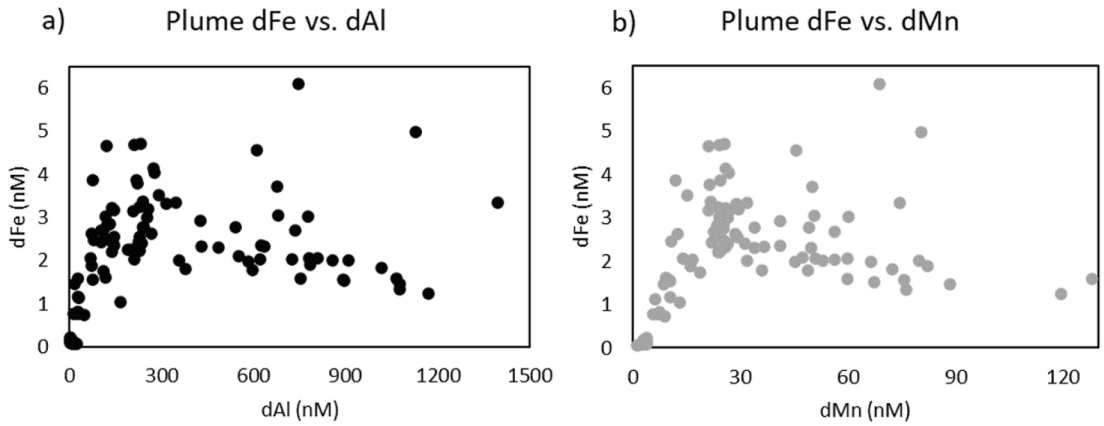

Fig. 17. Dissolved Fe as a function of a) dAl and b) dMn in the Copper River plume study (summer 2019).

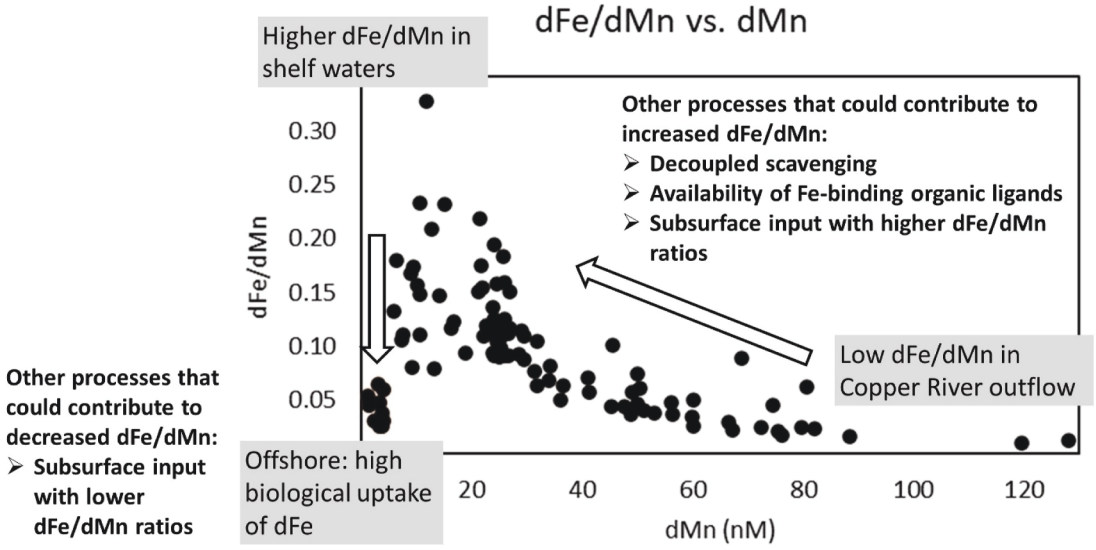

Fig. 18. dFe/dMn ratio plotted as a function of dMn for the Copper River plume study (summer 2019).

dFe tended to be more (or less) abundant relative to dMn. In higher salinity (>31.75) offshore waters, the ratio of dFe to dMn is low and less variable (0.03–0.06) providing an endmember where exceedingly low dFe concentrations (due to biological uptake and lack of additional input) drive the ratio down. The low ratios at high dMn values provide an endmember for a fresh Copper River plume (under high riverine input and spring tide conditions), where the low dFe:dMn ratios (0.01–0.02) are driven by the high input of dMn by the Copper River together with the capping of dFe concentrations by what is likely a combination of processes including particle scavenging, the low availability of Fe-binding organic ligands, and greater biological uptake. A third endmember is mid-salinity shelf waters (~28–31), where the ratio of dFe to dMn reaches its maximum (~0.25), suggesting high concentrations of Fe-binding organic ligands that help stabilize dFe, and an Fe source (such as suspended particles; e.g., Lippiatt et al., 2010) that can serve as a ready source of additional Fe as dFe is removed by biological uptake. A schematic diagram of processes that likely drive dFe:dMn ratios over the shelf is presented in Fig. 19.

5. Conclusions

Freshwater input from rivers appears to be the main source of dissolved Al and Mn to the surface waters of the NGA LTER study region. The NGA also receives large amounts of freshwater input from small discharges, but little is known about the concentrations of these metals in smaller streams, or the degree of removal that occurs at the freshwater/seawater interface. Riverine input varies seasonally with cycles of precipitation and glacial melt, reaching peak runoff observed in late summer/early autumn when discharge rates may be up to two times higher compared to rates observed in other seasons. Surface distributions of dAl and dMn reflected these seasonal patterns throughout the study region (Kodiak, Seward, and Middleton Lines) exhibiting concentrations that were higher on average during fall (high glacial melt) than spring (very low melt), and that were less pronounced with distance from the Copper River outflow, the major point source of fresh water in this region. Inshore/offshore gradients were commonly observed on all transects throughout the 2018–2019 field seasons, with higher dAl and dMn concentrations inshore (within ACC waters) that decreased off the shelf to consistently low values (≤10 nM dAl and <1–4 nM dMn). Coastal circulation (the ACC) keeps freshwater input constrained to the inner shelf, and advects surface water from the northwest region of the study area (MID Line) to the southeast (KOD Line). Along the ACC path, linear correlations between salinity and dissolved Al and Mn exhibited diminishing slopes with distance from the Copper River outflow. This decrease reflects removal of both metals via particle scavenging as well as input of freshwater into the ACC from small rivers and streams, likely providing lower input of dAl and dMn than the Copper River and diluting its signal. The dAl and dMn surface data from

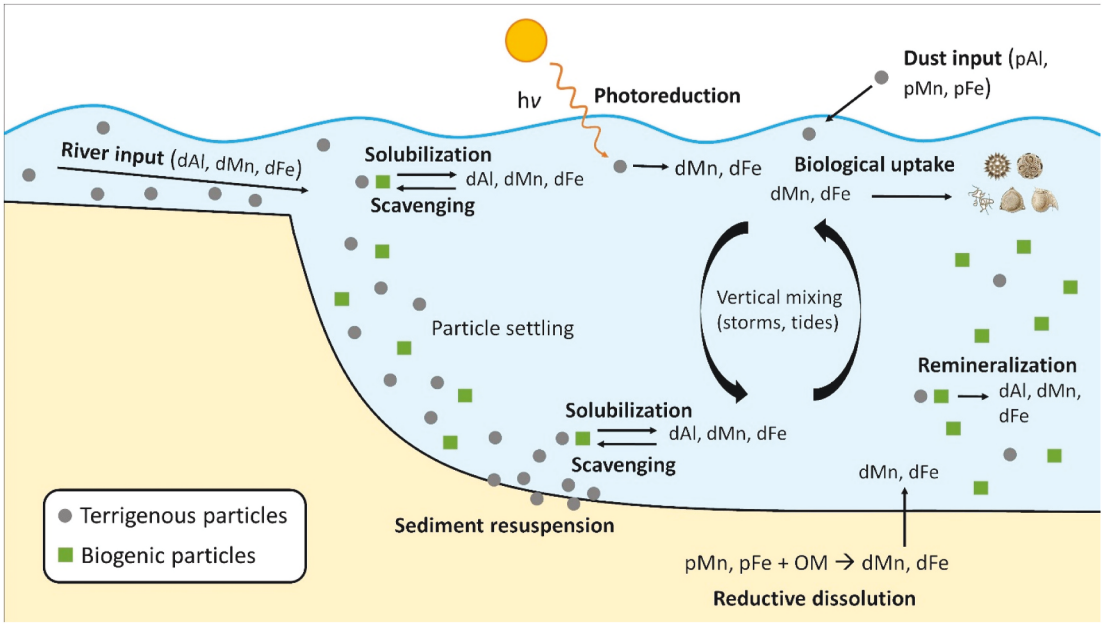

Fig. 19. Diagram illustrating processes affecting dAl, dMn, and dFe distributions throughout the water column.

the Copper River plume study (summer 2019) underscored the patchiness in the distribution of dissolved constituents within NGA surface shelf waters, which arises from the various processes that lead to the mixing of shelf waters and HNLC offshore waters.

Seasonal sampling near the Copper River outflow allowed us to estimate the residence times of dAl and dMn on a seasonal basis relative to input of fresh water by the Copper River plume. Residence times for both metals were on the order of days to months, which are reasonable given this region is rich in particles and both metals are particle reactive.

Vertical profiles from stations across the shelf provided some data suggesting sedimentary input to subsurface waters, and to surface waters over banks. Sedimentary inputs were more clearly observed for dMn over Albatross Bank in spring and summer, and over Tar Bank during spring when surface waters in the NGA were less impacted by freshwater input.

One of the goals of the NGA LTER site is to investigate how intense environmental variability can lead to ecosystem resilience. Overall, the wide ranges of concentrations observed for dAl and dMn suggest that inputs of dFe are highly spatially and temporally variable, contributing to the notion that the NGA naturally experiences intense environmental variability.

6. Data availability statement

Trace metal and CTD data described above are available through DataONE. Data associated with this article can be accessed at https://search.dataone.org/view/10.24431%2Frw1k459 (CTD data), https://search.dataone.org/view/10.24431%2Frw1k594 (dFe), and https://search.dataone.org/view/10.24431%2Frw1k584 (dAl and dMn).

Declaration of competing interest

The authors declare that they have no known competing financial interests or personal relationships that could have appeared to influence the work reported in this paper.

Acknowledgements

We thank the captains and crews of Tiglax, Sikuliaq, and Woldstad for their assistance on cruises. We also thank Mette Kaufman for help with the towfish, and Rachel Potter for providing the map shown in Fig. 2. In addition, we would like to acknowledge USGS for river discharge data and NOAA for tide data. We also thank the reviewers for thoughtful comments that improved the manuscript. This work was supported by the National Science Foundation grant OCE-1656070.

Appendix A. Supplementary data

Supplementary data to this article can be found online at https://doi.org/10.1016/j.dsr2.2021.104952.

References

Aguilar-Islas, A.M., Bruland, K.W., 2006. Dissolved manganese and silicic acid in the Columbia River plume: a major source to the California current and coastal waters off Washington and Oregon. Mar. Chem. 101, 233–247.
Aguilar-Islas, A.M., Séguret, M.J.M., Rember, R., Buck, K.N., Proctor, P., Mordy, C.W., Kachel, N.B., 2016. Temporal variability of reactive iron over the Gulf of Alaska shelf. Deep-Sea Research II 132, 90–106.
Beamer, J.P., Hill, D.F., Arendt, A., Liston, G.E., 2016. High-resolution modeling of coastal freshwater discharge and glacier mass balance in the Gulf of Alaska watershed. Ware Resources Research 52, 3888–3909.
Brown, M.T., Bruland, K.W., 2008. An improved flow-injection analysis method for the determination of dissolved aluminum in seawater. Limnol Oceanogr. Methods 6, 87–95.
Brown, M.T., Bruland, K.W., 2009. Dissolved and particulate aluminum in the Columbia River and coastal waters of Oregon and Washington: behavior in near-field and far-field plumes. Estuarine. Coastal and Shelf Science 84, 171–185.
Brown, M.T., Lippiatt, S.M., Bruland, K.W., 2010. Dissolved aluminum, particulate aluminum, and silicic acid in the northern Gulf of Alaska coastal waters: glacial/riverine inputs and extreme reactivity. Mar. Chem. 122, 160–175.
Bruland, K.W., Lohan, M.C., 2003. Controls of trace metals in seawater. In: Turekian, K. K., Holland, H.D. (Eds.), Treatise on Geochemistry, first ed. Elsevier Science, pp. 23–47.
Buck, K.N., Lohan, M.C., Carolyn, C.J.M., Bruland, K.W., 2007. Dissolved iron speciation in two distinct river plumes and an estuary: implications for riverine iron supply. Limnol. Oceanogr. 52 (2), 843–855.
Cheng, W., Hermann, A.J., Coyle, K.O., Dobbins, E.L., Kachel, N.B., Stabeno, P.J., 2012. Macro- and micro-nutrient flux to a highly productive submarine bank in the Gulf of Alaska: a model-based analysis of daily and interannual variability. Prog. Oceanogr. 101, 63–77.
Froelich, P.N., Klinkhammer, G.P., Bender, M.L., Luedtke, N.A., Heath, G.R., Cullen, D., Dauphin, P., 1979. Early oxidation of organic matter in pelagic sediments of the eastern equatorial Atlantic: suboxic diagenesis. Geochem. Cosmochim. Acta 43, 1075–1090.
Gibson, W.M., 1960. Submarine topography in the Gulf of Alaska. Bull. Geol. Soc. Am. 71, 1087–1108.
Guieu, C., Martin, J.M., 2002. The level and fate of metals in the Danube River plume. Estuarine,. Coastal and Shelf Science 54, 501–512.

Hill, D.F., Bruhis, N., Calos, S.E., Arendt, A., Beamer, J., 2015. Spatial and temporal variability of freshwater discharge into the Gulf of Alaska. J. Geophys. Res.: Oceans 120, 634 646.
Hydes, D.J., 1979. Aluminum in seawater: control by inorganic processes. Science 205, 1260 1262.
Jones, M.R., Luther III, G.W., Tebo, B.M., 2020. Distribution and concentration of soluble manganese(II), soluble reactive Mn(III)-L, and particulate MnO_2 in the Northwest Atlantic Ocean. Mar. Chem. 226, 103858.
Lagerloef, G.S.E., 1995. Interdecadal variations in the Alaska gyre. J. Phys. Oceanogr. 25, 2242 2258.
Ladd, C., Mordy, C.W., Kachel, N.B., Stabeno, P.J., 2007. Northern Gulf of Alaska eddies and associated anomalies. Deep Sea Res. I 54, 487 509.
Landing, W.M., Bruland, K.W., 1987. The contrasting biogeochemistry of iron and manganese in the Pacific Ocean. Geochem. Cosmochim. Acta 51, 29 43.
Lippiatt, S.M., Lohan, M.C., Bruland, K.W., 2010. The distribution of reactive iron in northern Gulf of Alaska coastal waters. Mar. Chem. 121, 187 199.
McAlister, J., Orians, K., 2012. Calculation of river-seawater endmembers and differential trace metal scavenging in the Columbia River plume. Estuarine. Coastal and Shelf Science 99, 31 41.
Minami, T., Konagaya, W., Zheng, L., Takano, S., Sasaki, M., Murata, R., Nakaguchi, Y., Sohrin, Y., 2015. An off-line preconcentration system with ethylenediaminetriacetate chelating resin for the determination of trace metals in seawater by high-resolution inductively coupled plasma mass spectrometry. Anal. Chim. Acta 854, 183 190.
Orians, K.J., Bruland, K.W., 1986. The biogeochemistry of aluminum in the Pacific Ocean. Earth Planet Sci. Lett. 78, 397 410.
Rember, R., Aguilar-Islas, A.M., Domena, V., 2016. Distribution and abundance of select trace metals in Chukchi and Beaufort Sea ice. OCS Study BOEM 2016 2079.
Ren, J.L., Zhang, J., Li, J.B., Yu, X.Y., Liu, S.M., Zhang, E.R., 2006. Dissolved aluminum in the yellow sea and east China sea Al as a tracer of changjiang (Yangtze River) discharge and kuroshio incursion. Estuarine. Coastal and Shelf Science 68, 165 174.
Roitz, J.S., Flegal, A.R., Bruland, K.W., 2002. The biogeochemical cycling of manganese in San Francisco Bay: temporal and spatial variations in surface water concentrations. Estuarine,. Coastal and Shelf Science 54, 227 239.
Royer, T.C., 1975. Seasonal variations of waters in the northern Gulf of Alaska. Deep-Sea Res. 22, 403 416.
Royer, T.C., 1981. Baroclinic transport in the Gulf of Alaska Part II. A fresh water driven coastal current. J. Mar. Res. 39, 251 266.
Royer, T.C., Emery, W.J., 1987. Circulation in the Gulf of Alaska, 1981. Deep-sea Research Part A. Oceanographic Research Papers 34, 1361 1377.
Rue, E.L., Bruland, K.W., 1995. Complexation of iron(iii) by natural organic ligands in the central north pacific as determined by a new competitive ligand equilibration/ adsorptive cathodic stripping voltammetric method. Mar. Chem. 50, 117 138.
Rutgers Van Def Loeff, M.M., Meadows, P.S., Allen, J.A., 1990. Oxygen in pore waters of deep-sea sediments. Philosophical transactions of the royal society of london. Series A. Mathematical and Physical Sciences 331, 69 84.
Schumacher, J.D., Stabeno, P.J., Roach, A.T., 1989. Volume transport in the Alaska coastal current. Continent. Shelf Res. 9, 1071 1083.
Shiller, A.M., 1997. Dissolved trace elements in the Mississippi River: seasonal, interannual, and decadal variability. Geochem. Cosmochim. Acta 61, 4321 4330.
Spotila, J.A., Buscher, J.T., Meigs, A.J., Reiners, P.W., 2004. Long-term glacial erosion of active mountain belts: example of the Chugach-St. Elias Range, Alaska. Geology 32, 501 504.
Strom, S.L., Olson, M.B., Macri, E.L., Mordy, C.W., 2006. Cross-shelf gradients in phytoplankton community structure, nutrient utilization, and growth rate in the coastal Gulf of Alaska. Mar. Ecol. Prog. Ser. 328, 75 92.
Strom, S.L., Macri, E.L., Fredrickson, K.A., 2010. Light limitation of summer primary production in the coastal Gulf of Alaska: physiological and environmental causes. Mar. Ecol. Prog. Ser. 402, 45 57.
Sunda, W.G., Huntsman, S.A., 1988. Effect of sunlight on redox cycles of manganese in the southwestern Sargasso Sea. Deep-Sea Res. 35, 1297 1317.
Sunda, W.G., Huntsman, S.A., 1994. Photoreduction of manganese oxides in seawater. Mar. Chem. 46, 133 152.
Taylor, S. R. Abundance of chemical elements in the continental crust: a new table. Geochem. Cosmochim. Acta 28, 1273 1285.
Twining, B.S., Baines, S.B., 2013. The trace metal composition of marine phytoplankton. Annual Review of Marine Science 5, 191 215.
Waite, J.N., Mueter, F.J., 2013. Spatial and temporal variability of chlorophyll-a concentrations in the coastal Gulf of Alaska, 1998-2011, using cloud-free reconstructions of SeaWiFS and MODIS-Aqua data. Prog. Oceanogr. 116, 179 192.
Weingartner, T.J., Danielson, S.L., Royer, T.C., 2005. Freshwater variability and predictability in the Alaska coastal current. Deep-Sea Research II: Topical Studies in Oceanography 52, 169 191.
Wu, J., Luther III, G.W., 1994. Size-fractionated iron concentrations in the water column of the western North Atlantic Ocean. Limnol. Oceanogr. 39 (5), 1119 1129.
Yang, S., Sanudo-Wilhelmy, S.A., 1998. Cadmium and manganese distributions in the Hudson River estuary: interannual and seasonal variability. Earth Planet Sci. Lett. 160, 403 418.
Yang, L., Nadeau, K., Meija, J., Grinberg, P., Pagliano, E., Ardini, F., Grotti, M., Schlosser, C., Streu, P., Achterberg, E.P., Sohrin, Y., Minami, T., Zheng, L., Wu, J., Chen, G., Ellwood, M.J., Turetta, C., Aguilar-Islas, A., Rember, R., Sarthou, G., Tonnard, M., Planquette, H., Matousek, T., Crum, S., Mester, Z., 2018. Inter-laboratory study for the certification of trace elements in seawater certified reference materials NASS-7 and CASS-6. Anal. Bioanal. Chem. 410, 4469 4479.
Zimmermann, M., Prescott, M.M., 2015. Smooth sheet bathymetry of the central Gulf of Alaska. NOAA technical memorandum NMFS-AFSC-287.